

An Integrated Framework of Artificial Intelligence and Genetic Algorithm for Optimization of Shell and Tube Heat Exchanger under Uncertainty



By

Zahid Ullah

**School of Chemical and Materials Engineering
National University of Sciences and Technology
H-12, Islamabad, Pakistan
November 2021**

An Integrated Framework of Artificial Intelligence and Genetic Algorithm for Optimization of Shell and Tube Heat Exchanger under Uncertainty



Name: Zahid Ullah

Reg. No.: Fall-2019-MS-PSE-02-00000320548

**This work is submitted as partial fulfillment of the requirement for the
degree of**

MS in Process Systems Engineering

Supervisor Name: Dr. Iftikhar Ahmad

**School of Chemical and Materials Engineering (SCME)
National University of Sciences and Technology (NUST)**

H-12, Islamabad, Pakistan

November 2021

DEDICATION

To my very Supportive, Loving, and Caring

Family

ACKNOWLEDGMENTS

First and foremost, praise is to Almighty Allah Who bestowed upon me with His blessings and guided me in completing this task. It would not have been possible without the support of family. The foremost help and support of several individuals/colleagues who were available all the time and helped me with their suggestions to compile this work.

I would like to show my profound appreciation to my supervisor, **Dr. Iftikhar Ahmad**, for his timely advice, helpful and practical attitude throughout this task. It is worth noting here that it is only his relentless pursuit that has led to the completion of my job. There were several obstacles and challenges during my research job, yet he stayed not always available but pushed me to do the task more effectively.

I am also thankful to my Guidance and Examination Committee (GEC) Members **Dr. Muhammad Ahsan**, and **Dr. Muhammad Nouman Aslam Khan** for their valuable guidance. Besides, the contributions of several postgraduate students are acknowledged, they have been a great source of support and motivation.

ABSTRACT

To reduce energy consumption, an energy-efficient process is vital. Heat exchanger is one of the most abundant used equipment in the process industry. The shell and tube heat exchanger (STHE) is widely used in chemical, petroleum, and other process industries. In the literature, a lot of work has been done on the design and optimization of the STHE using different optimization methods. Although no one is focusing on the optimization of shell and tube heat exchangers under uncertain process conditions. The current work developed an Integrated Framework of Artificial Intelligence and Genetic Algorithm for STHE to predict the optimum inlet stream mass flow rates in the presence of uncertainty in process conditions. Using optimized industrial data, the STHE model was regenerated in Aspen EDR. The COM server was used to build the interface between Aspen HYSYS and MATLAB. The data set was generated by inserting the variation of ± 1 , ± 2 , ± 3 , ± 4 , and ± 5 in the crude oil composition as well as in the inlet temperature and pressure of cold crude and hot kerosene oil. The optimum mass flow rate for each variation was determined using a single objective genetic algorithm. A total of 400 samples were generated, 70% were used for the training of feed-forward neural network and the remaining samples were equally divided for the validation and testing of the model. The proposed artificial neural network (ANN) model has a correlation coefficient of 0.999. The high accuracy and robustness of the ANN model, make it suitable for real-time industrial application, to reduce energy consumption.

KEYWORDS:

Shell and tube heat exchanger, artificial neural network, Genetic algorithm, Optimization, uncertainty

TABLE OF CONTENTS

DEDICATION	i
ACKNOWLEDGMENTS	ii
ABSTRACT	iii
KEYWORDS:	iii
LIST OF FIGURES	vi
LIST OF TABLES	viii
NOMENCLATURE	ix
CHAPTER 1: INTRODUCTION	1
1.1. Background	1
1.2. Shell and Tube Heat Exchanger	2
CHAPTER 2: LITERATURE REVIEW	5
2.1. Literature Review	5
2.2. Objectives	13
2.3. Research Justification	13
2.4. Thesis Outline	14
CHAPTER 3: OVERVIEW OF MODELS	15
3.1. Aspen EDR Model	15
3.1.1. Design Mode	15
3.1.2. Rating / Checking Mode	15
3.1.3. Simulation Mode	15
3.1.4. Find Fouling Mode	15
3.2. Genetic Algorithm	18
3.2.1. Background	18
3.2.2. Genetic Algorithm Operators:	18
a. Initial Population	18
b. Selection	19
c. Crossover	20
d. Mutation	21
3.3. Artificial Neural Network	24
3.3.1. Background	24

3.3.2. ANN Architecture and Training Process.....	24
a. Input layer	24
b. Hidden, intermediate, or invisible layers	24
c. Output layer	24
3.4. Exergy Analysis.....	26
CHAPTER 4: METHODOLOGY	28
4.1. Overview of Methodology	28
4.2. Process Data.....	29
4.3. Aspen EDR Model Development.....	31
4.3.1. Simple Heat Exchanger Models	31
4.3.2. Detail Model Development.....	33
4.4. Aspen HYSYS and MATLAB Interfacing	34
.....	35
4.5. Single objective Genetic algorithm for optimization	35
4.6. Data generation	36
4.7. Artificial neural network (ANN) model training and validation	37
CHAPTER 5: RESULTS AND DISCUSSION.....	39
5.1. Optimization through Genetic Algorithm	39
5.2. Prediction through ANN.....	41
5.3. Exergy Analysis.....	46
5.5. Graphical User Interface (GUI).....	50
CONCLUSION.....	51
FUTURE RECOMMENDATION	52
REFERENCE:.....	53

LIST OF FIGURES

Figure 1: Cross-sectional view of shell and tube heat exchanger	3
Figure 2: Schematic of fluid flow through small to large baffle cuts and spacing	4
Figure 3: Schematic of two-point crossover	6
Figure 4: Schematic diagram of cuckoo-search algorithm.....	8
Figure 5: Architecture of Artificial Neural Network used in [3a].....	11
Figure 6: Schematic of experimental setup used in 43.....	12
Figure 7: Calculation Modes in Aspen Exchanger Design and Rating Tool	16
Figure 8: Mechanism of roulette wheel in genetic algorithm	20
Figure 9: Single-point and double-point crossover are two prominent crossover strategies in GA.	21
Figure 10: After the crossover phase, the mutation operator changes one or more genes in the children's solutions	22
Figure 11: Flow diagram of Genetic Algorithm.....	23
Figure 12: General architecture of ANN model.....	25
Figure 13: Schematic of Shell and tube heat exchanger	26
Figure 14: Flow diagram of the present research work.....	29
Figure 15: Shell and tube heat Exchanger model.....	30
Figure 16: Selection of STHE Model in Aspen HYSYS	31
Figure 17: Connections of stream in STHE model	32
Figure 18: Entering input parameter using worksheet page.....	32
Figure 19: Entering inputs for the STHE model	33
Figure 20: Entering geometrical information for STHE model in Aspen EDR.....	34
Figure 21: Proposed ANN model Architecture.....	37
Figure 22: Actual vs. predicted value based on ANN model.....	38

Figure 23: Average Outlet temperature value	42
Figure 24: Average STHE effectiveness	42
Figure 25: Comparison of Kerosene outlet temperature obtained through SR, GA, and ANN models ...	43
Figure 26: Comparison of STHE effectiveness obtained through SR, GA, and ANN models.....	43
Figure 27: Average Exergy loss comparison between ANN and straight run	47
Figure 28: Exergy Efficiency predicted by the straight run and ANN model.....	47
Figure 29: ANN-based Graphical user interface.....	50

LIST OF TABLES

Table 1: Summary of various optimization based for studies in STHE.....	10
Table 2: Exchanger Geometry Details Requirement.....	17
Table 3: Design parameters of STHE	30
Table 4: Ten Data sample of generated data	36
Table 5: Comparison between straight run and GA.....	40
Table 6: Comparison between SR, GA and ANN for kerosene outlet temperature.....	44
Table 7: Comparison between SR, GA, and ANN-based prediction of STHE effectiveness.....	45

NOMENCLATURE

Heat Exchanger (HE)

Artificial Intelligence (AI)

Machine Learning (ML)

Artificial Neural Network (ANN)

Shell and Tube Heat Exchanger (STHE)

Aspen Exchanger Design Rating tool (EDR)

Genetic Algorithm (GA)

Straight Run (SR)

Barrels per day (BPD)

Biogeography-based (BBO)

Harmony search algorithm (HSA)

Artificial Bee Colony (ABC)

Graphical User Interface (GUI)

Particle swarm optimization (PSO)

Crude distillation unit (CDU)

Cuckoo-search-algorithm (CSA)

Multi-output feed-forward neural network (MFFNN)

CHAPTER 1: INTRODUCTION

1.1. Background

The continues depletion of global energy supplies as a result of growing human consumption has resulted in a reduction in natural energy resources such as combustible gas, oil, and coal. Currently, Fossil fuels are the most important energy resource and their consumption is increasing rapidly [1]. The statistics show that the worldwide use of petroleum-based fuel is projected to increase from 85.6 million barrels per day (BPD) in 2008 to 112.2 million (BPD) by 2035 [2]. In order to bridge the energy supply-demand gap, energy production must be enhanced at the same pace as its consumption. One of the most energy-intensive industries is the process industry. It is critical to have an efficient energy process in order to decrease energy usage. In refineries, the product(s) from the distillation column is used for preheating the crude oil. This process is done in series of heat exchangers; in this way the product heat is utilized to decrease the furnace heat duty. The best pre-heat train or exchanger network design will significantly reduce the duty of the furnace [3].

Heat exchangers are one of the most essential equipment in chemical processes for energy and heat transfer. Because of their benefits over traditional energy analysis methods, the idea of exergy is gaining traction among researchers for energy efficient heat exchanger design. A heat exchanger is a piece of equipment that uses thermal contact to transfer heat between hot and cold streams [4]. Heat exchangers are one of the most commonly used equipment in process industries such as chemical, petroleum, and others. There is generally no outside heat and work connection in heat exchangers. The heating or cooling of a flowing fluid of interest, including the evaporation or condensation of single or multicomponent fluid streams, are common uses. In other cases, the goal could be to recover or reject heat, or to sterilize, pasteurize, distillate, crystallize fractionate, concentrate, or regulate a process [5]. Only a few heat exchangers have direct contact between the fluids transferring heat while in most of heat exchangers, heat transfer between fluids occurs in a transitory way through a dividing wall or into or out of a wall [6]. Among other heat exchangers, shell and tube heat exchangers (STHE) are the most widely used, accounting for more than 65% of the exchanger in chemical process industries, This is because

STHE have a high surface area per unit volume, with 700 m²/m³ for gases and 300 m²/m³ for liquids [7].

1.2. Shell and Tube Heat Exchanger

Shell-and-tube heat exchangers (STHEs) are the most typical form of heat exchanger, and they can operate at a wide range of temperatures and pressures. They offer higher heat transfer surface to volume ratios than double-pipe heat exchangers, and they're simple to make in a wide range of sizes and flow configurations. They can withstand high pressures, and their design allows for easy disassembling for routine maintenance and cleaning [8,9]. STHEs are widely utilized in a variety of sectors due to their reduced production costs, ease of cleaning, and perceived flexibility when compared to conventional heat exchangers. Refrigeration, chemical processes, heating and air conditioning, power generation, and manufacturing all employ STHEs [10–12]. The double-pipe design is extended with a STHE. A STHE consists of a collection of pipes or tubes encased inside a cylindrical body, rather than a single pipe within a larger pipe. One fluid circulates through the tubes, while another circulates between the tubes and the shell [13,14]. The main components of the STHE shown in [Figure 1](#) are as follows,

- Shell
- Tube
- Baffles
- Channel
- Channel cover
- Shell cover
- Tube sheet
- Nozzles

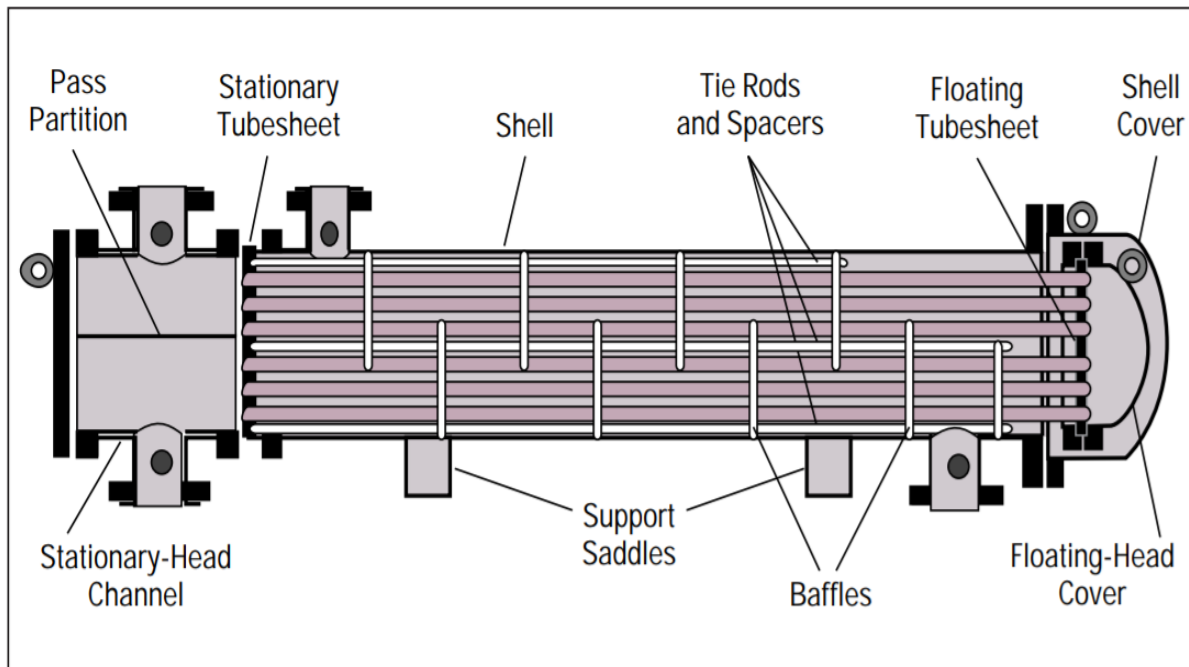


Figure 1: Cross-sectional view of shell and tube heat exchanger

The performance or effectiveness of the STHE depends on various influencing factors including heat exchanger length, drop in pressure, baffle type, tube and shell side flow rates, turbulence, and fouling [15–17].

Turbulence: With increase in the intensity level turbulence, the resistance in the flow of fluid can be increased, in this way the heat transfer can be enhanced effectively [18].

Pressure drops: With upsurge in the pressure drop, the rate of transfer of energy also increases but it consumes more energy. To cope with this drawback, the pressure drop value is optimized to achieve the optimized results of both heat transfer rate and consumption of energy or power [19,20].

Heat Transfer Coefficient: With increase in the heat transfer coefficient the rate of heat transfer increases. The coefficient of heat transfer is increased by enhancing the flow rate at the tube and shell sides, opposite flow path or configuration, pitch and diameter of a coil [21,22].

Fouling: For achieving the better performance of the heat exchanger, fouling should be lowest. In the heat exchanger system, fouling is dependent on the composition of the fluid, material of

the pipe, and temperature of the wall [23,24].

Heat Exchanger Length: The length of the heat exchanger affects the performance. With increase in the length of heat exchanger, the heat transfer coefficient to pressure drop ratio decreases and vice versa [25].

Type of Baffles: Baffles are the key elements that are considered in the design of STHE. Baffles are used to generate the disorder in the stream, support the bundle of tubes, and to upsurge the velocity of the fluid. Different baffle types are used in the STHEs with different cut-ratation. Segmental, disc, ring, helical, and flower type baffles are various types of the baffles [26,27]. The cut-ratation in the baffles ranges from the small baffle cut to large baffle cut and spacing, as shown in the [Figure 2](#).

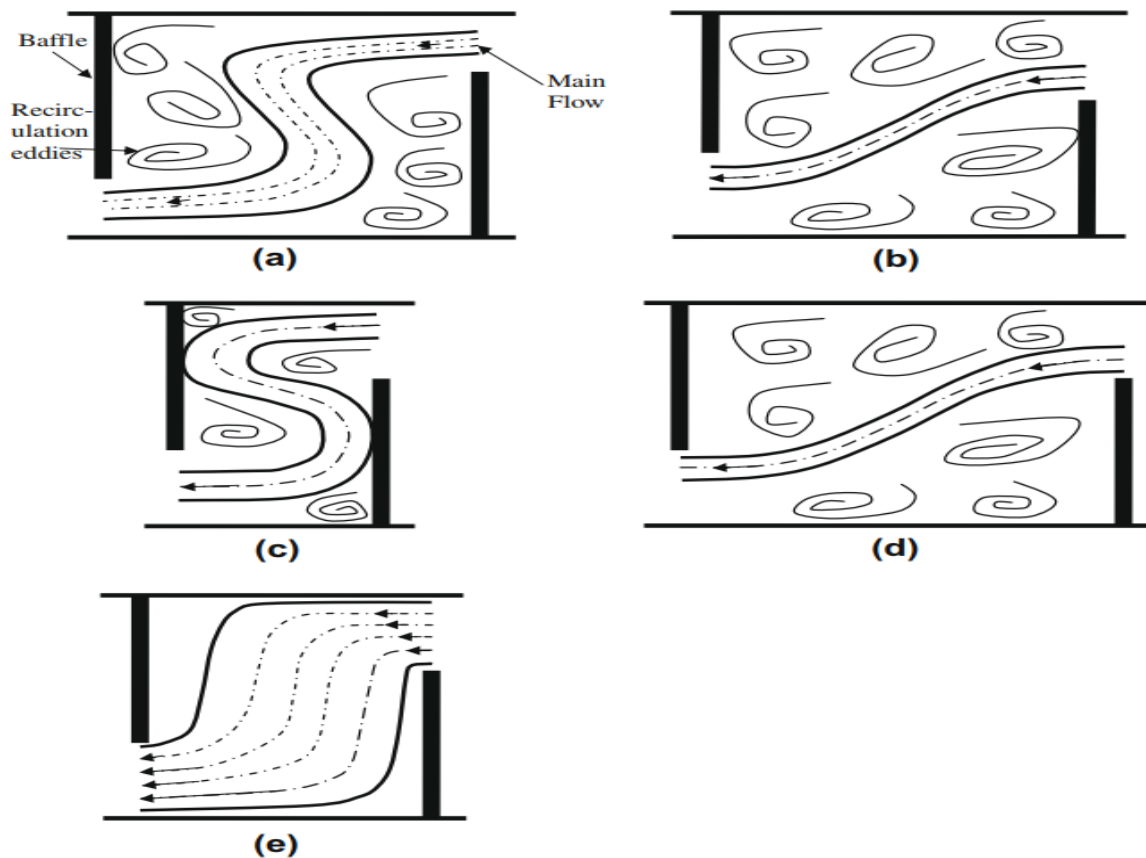


Figure 2: Schematic of fluid flow through small to large baffle cuts and spacing

CHAPTER 2: LITERATURE REVIEW

2.1. Literature Review

The process industry is one of the most energy-intensive industries. It is critical to have an efficient energy process in order to reduce energy consumption. In the process sector, heat exchangers are one of the most used pieces of equipment. Among other STHE is the most widely used in process industries. This is because STHE have a high surface area per unit volume [7]. Owing to the ever-growing need of STHE in industrial uses so every consumer is keen on its most optimum operation whereas this goal can be accomplished with various methodologies. The efficiency of heat exchanger is highly dependent on the temperature of cold and hot fluid at the inlet. Whereas the temperature at inlet depends upon the flow rate of associated fluid stream such as temperature can be controlled by controlling fluid flow rate. By reducing flow rate, the pressure drop increases thus require higher pumping power, so a reasonable tradeoff is required [28].

Although many research studies on the STHE have been published, most of them focus on the design and optimization. For instance, [29] proposed the optimal design of STHE using genetic algorithm (GA), where the objective function was cost minimization. In this study, the core objective was to estimate the heat transfer area first (minimum), since it manages the total cost of the STHE. LMTD method was used to compute the heat transfer area. The proposed optimization technique is employed to the STHE optimal design by changing various parameters such as tube outside diameter, tube layout, outer shell diameter, and baffle spacing. The authors concluded that the proposed method has successfully examined the optimal scheme of STHE as related to the conventional method. The schematic of two-point crossover proposed in this study is shown in [Figure 3](#).

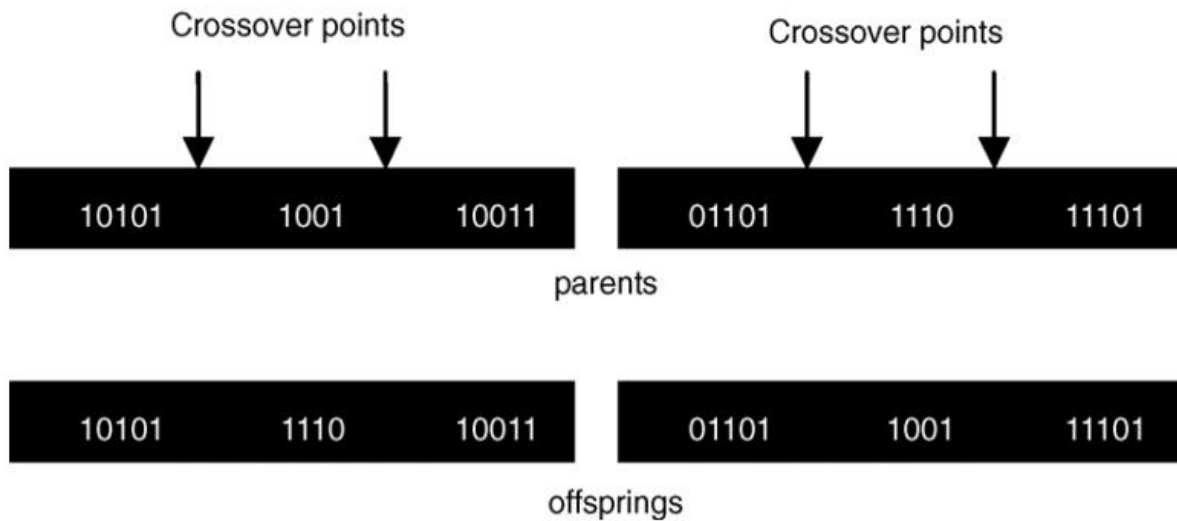


Figure 3: Schematic of two-point crossover

In another study by [30], developed a harmony search algorithm (HSA) for the optimal design of STHE. The objective function was total cost minimization. In this study, first of all, the global sensitivity analysis method was used to determine the impact of various geometrical parameters on the total cost of STHE. Once the non-influential parameters were identified, the HSA was used for the optimization of most influential parameters on cost of STHE. Moreover, the proposed method was compared with GA based optimization method for performance evaluation. The authors found that HSA optimization technique performed well with high convergence accuracy.

Furthermore, [31] used a multi-objective optimization strategy for the prime design of STHE. The novel fast and elitist non-dominated sorting genetic algorithm (NSGA II) has been proposed in this study for the optimization of heat transfer area and the pumping power of STHE. Tube layout pattern, baffle spacing, tube-to-baffle diameter, baffle cut, number of tube passes, shell-to baffle diameter, tube length, tube wall thickness, and tube outer diameter were considered as decision variables. With $A_o = 32.66 \text{ m}^2$ and $P_{s,t} = 193.25 \text{ W}$, a minimal cost of \$3391/year was achieved with Design 2.

Moreover, [32] proposed a multi-objective optimization model for an optimal design of STHE

using seven different design parameters. The different design parameters to be optimized include tube arrangement, tube diameter, tube number, baffle spacing ratio, and baffle cut ratio. Firstly, the STHE were modelled thermally using the e-NTU method followed by the implementation of other novel method for the estimation of pressure drop and heat transfer coefficient at the shell side. The main aim was to optimize the effectiveness as well as the cost of STHE. Therefore, for the estimating the maximum effectiveness and minimum cost of STHE, the genetic algorithm (GA) based optimization method (non-dominated sorting) was used. Moreover, the sensitivity analysis was performed to check the influence of various design parameters of the cost and effectiveness of the STHE. It was concluded by the authors that the tube length, tube pitch, tube number, and ratio of baffle spacing has great influence on the output parameters. By using the optimized values of these parameters, both the cost and effectiveness of STHE can be optimized.

In another study, the Cuckoo-search-algorithm was employed for the optimal design of STHE [33]. The objective function in this study was to minimize the total annual cost. The results reveal that by employing the CSA algorithm, energy may be saved by 77%. When compared to the results obtained by PSO and GA, the operational expenses may be lowered by 77 % and 48 %, respectively. In both situations, this is accomplished by increasing the number of tubes and lowering the heat exchanger length. The schematic diagram of cuckoo-search algorithm is shown in [Figure 4](#).

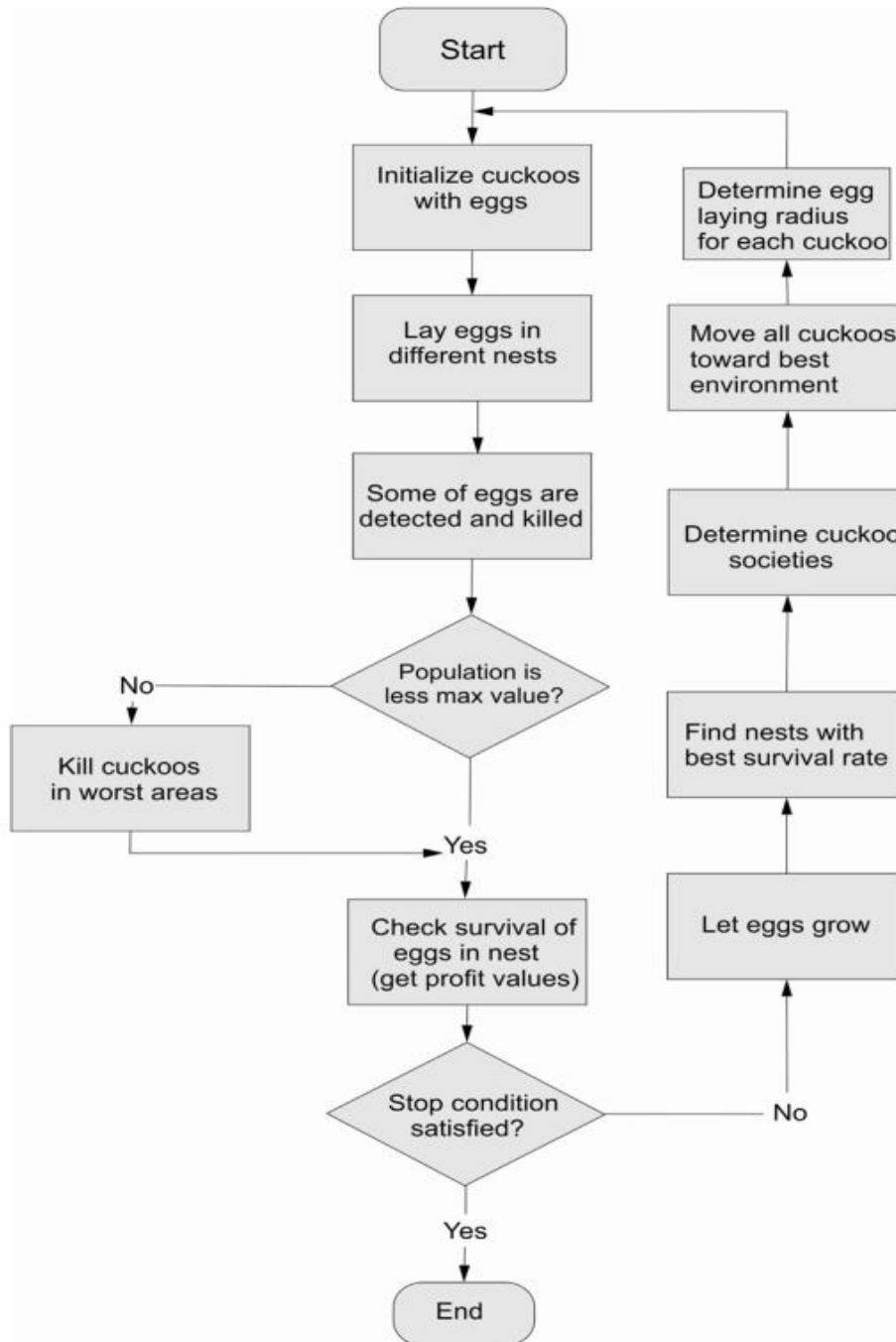


Figure 4: Schematic diagram of cuckoo-search algorithm

Authors in [34] used a novel optimization approach, Biogeography-based (BBO) algorithm, for the optimization of STHE. The aim was to minimize the cost of STHE. The authors concluded that the proposed method can successfully employed for the optimal design of STHE. As a consequence, capital expenditure was reduced by 14 percent, and operational expenses were reduced by 96 percent, resulting in a total cost reduction of 56.1 percent, demonstrating the suggested method's improvement potential.

In [35], a multi-objective optimization method, bat algorithm, was developed for the optimal design of STHE. The two objective functions were STHE effectiveness and total cost. The design parameters including baffle cuts, pitch, baffle spacing, and tube length were considered. For the verification of the proposed algorithm, a case study taken from the published research article has been analyzed. The results showed that the proposed novel bat algorithm performed well, and it was concluded that the cost is reduced by a maximum of 13.7 percent and a minimum of 9.2 percent using the bat algorithm's Pareto optimum solution. [Table 1](#) shows the summary of optimization methods used in shell and tube exchanger.

Furthermore, [40] used an ANN model for forecasting the heat transfer rates of STHE. For training the network, the back propagation algorithm was employed on the actual experimental data. The proposed ANN model contains two hidden layers, eight input variables, and three output variables. The inputs of the ANN model were tube diameter, baffle pitch, water, and oil Reynolds numbers. Rate of heat transfer and temperature differences at both sides were used as output of the model. Results showed that the proposed model achieved high performance with relative error of less than 2 percent. The schematic of the neural network algorithm used in this study is shown in [Figure 5](#).

Table 1: Summary of various optimization based for studies in STHE

S.No	Author	Summary	Optimization Method	Objective Function	Reference
1	Selbas et al.	Design of STHE using GA from economic point of view	Genetic Algorithm	Total Cost	[29]
2	Fesanghary et al.	Design optimization of STHE using global sensitivity analysis and HSA	Harmony search algorithm	Total Cost	[30]
3	Fettaka et al.	Design of STHE using multi-objective optimization	Non-dominated sorting genetic algorithm	Heat transfer area Pumping power	[31]
4	Sanaye et al.	Multi-objective optimization of STHE	Non-dominated sorting genetic algorithm	Effectiveness Total Cost	[32]
5	Asadi et al.	Economic optimization design of STHE by a CSO	Cuckoo-search-algorithm	Total annual Cost	[33]
6	Hadidi et al.	Design and economic optimization of STHE using BBO	Biogeography-based algorithm	Total Cost	[34]
7	Patel et al.	Design optimization of STHE using PSO technique	Particle swarm optimization	Total cost	[36]
8	Mirzaei et al.	Design and economic optimization of STHE using ABC algorithm	Artificial Bee Colony algorithm	Total cost	[37]
9	Tharakeshwar et al.	Multi-objective optimization using bat algorithm for STHE	Bat algorithm	Effectiveness Total Cost	[35]
10	Mirzaei et al.	Multi-objective optimization of STHE by constructal theory	Constructal theory	Effectiveness Total Cost	[38]
11	Mohanty	Application of firefly algorithm for design optimization of a STHE	Firefly algorithm	Total annual Cost	[39]

Similarly, [41] used an ANN model for the cost estimation of STHE prior to detailed designing phase. The proposed ANN model contains two hidden layers, five input variables, and one output variable. The inputs of the ANN model were tube pitch, tube diameter, shell diameter, red head

factor, and stationary head factor. While the output of the model was cost per exchanger area. Results showed that the proposed model performed well (correlation coefficient=0.97). The authors concluded that the use of their proposed model can reduce the variabilities in the estimation of cost of STHE and results in accurate cost estimation.

Furthermore, [42] employed an ANN model for forecasting the rate of heat transfer in STHE. The proposed ANN model contains two hidden layers, four input variables, and one output variable. Number of baffles, baffle pitch, and center diameter were used as an input while heat transfer rate is used as output of the model. Back propagation algorithm was used for training the model, which results in poor performance. Therefore, a novel teaching learning optimization model was employed to reduce the error. It was concluded that the proposed model showed good performance and can successfully predict the rate of heat transfer.

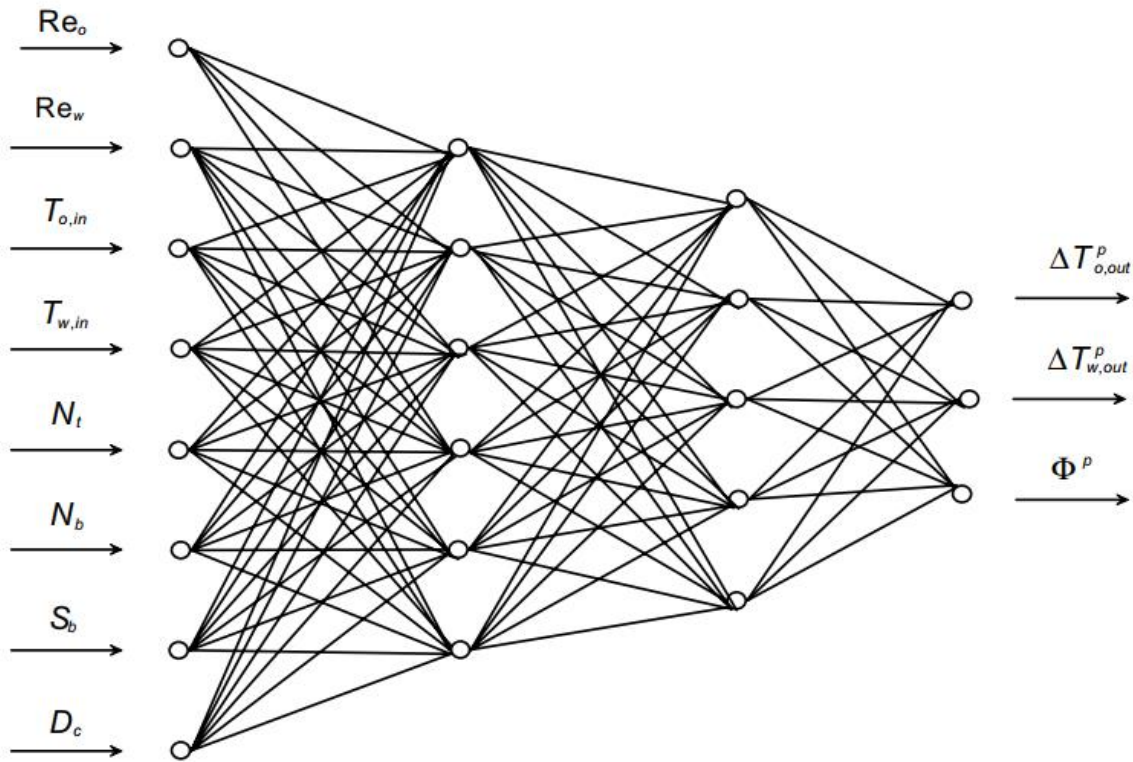


Figure 5: Architecture of Artificial Neural Network used in [3a]

For the prediction of thermal and hydrodynamic properties of the two different coolants used in STHE [43]. The proposed ANN model contains two hidden layers, four input variables, and two

output variables. In addition, the multi-objective optimization was used for maximizing the Nusselt number and minimizing the pressure drop. The proposed model performed well and obtained 0.09 difference between experimental and proposed study results, while that of 0.096 error for the drop in pressure. The schematic of experimental setup used in this study is shown in Figure 6.

In [44], used an ANN based model for the prediction of outlet temperature of STHE using industrial data. For training and testing, the back propagation algorithm was employed. Water inlet temperature, air inlet temperature, and mass flow rate were used as an input while water outlet temperature and air outlet temperature were used as output of the model.

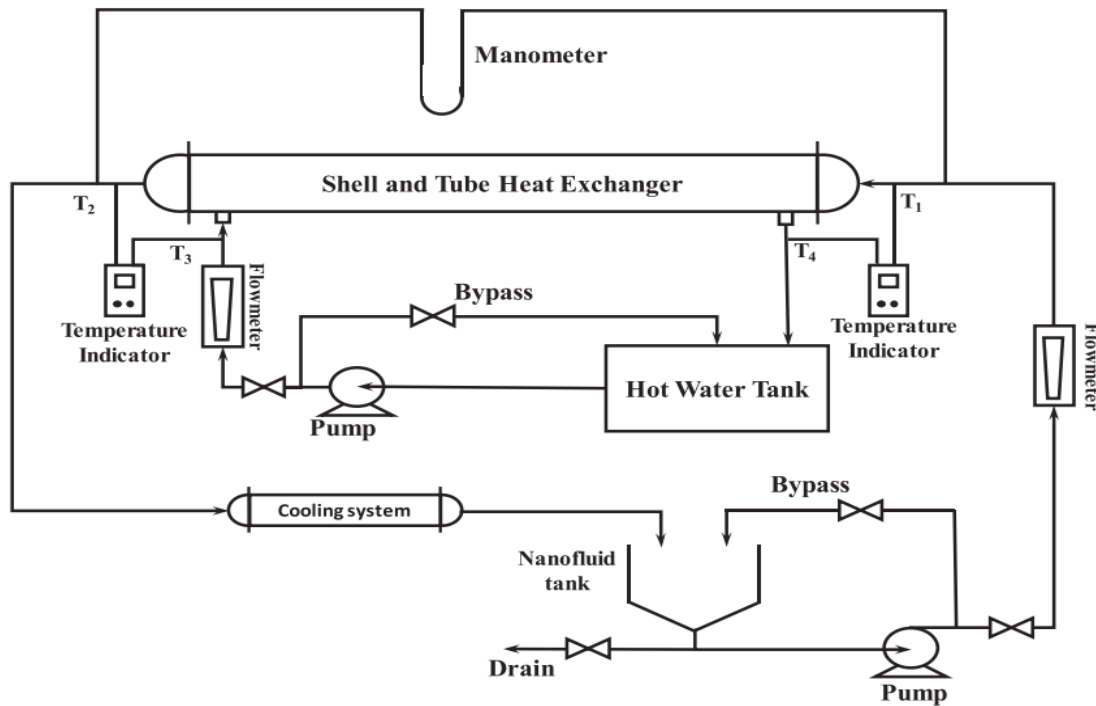


Figure 6: Schematic of experimental setup used in 43.

Although, many studies have been published on the design and modeling of STHE, no one has focused on the hybrid approach for the optimum operating condition of STHE under uncertain process condition. As the operation of a STHE under uncertain feed composition and process conditions causes low efficiency and wastage of a substantial amount of

energy. Therefore, the main aim of the present study is to develop structured neural network model which is based on the simulated data of the GA to locate the top-notch optimized process condition. Current study highlights the importance of heat exchangers design parameters and operating variables under uncertain conditions.

2.2. Objectives

The key objectives of the present study are given below:

- STHE thermal modeling in Aspen Exchanger design and rating environment.
- Interfacing of Aspen HYSYS and MATLAB software through COM server.
- Applying single objective optimization technique for the minimization of hot outlet stream temperature by manipulating the inlet streams mass flow rate under uncertainty in the crude composition and other process parameters (Crude temperature and pressure, kerosene temperature and pressure).
- Artificial Neural Network (ANN) model training and validation on the generated data from interfacing of Aspen HYSYS and MATLAB software.
- Exergy analysis and Comparison of the Exergy efficiency predicted by the straight run and ANN.
- Development of Graphical User Interface (GUI) based on the optimized ANN model that will used to predict the inlet stream mass flow rate under uncertainty in the crude composition and process conditions.

2.3. Research Justification

Pakistan has not yet achieved energy self-sufficiency and requires highly effective processing facilities. So, the application of artificial intelligence to such complex chemical processes will meet the national interest of energy saving. This research will greatly enhance the efficiency of the existing Heat exchanger units in local oil refineries. It will also pave the ways for application of artificial intelligence and process automation to industries which is the need for modern day concept of Industry 4.0.

- The model will provide a platform to design and optimize the STHE exchanger for real application in process industries.
- The project will pave ways in future for applying it to other industrial uncertainties problem like scheduling of raw material and product, estimation of product properties, optimization and control of important process parameters.

2.4. Thesis Outline

This thesis is ordered as follows, chapter 1 presents the introduction of the research topic, followed by the extensive literature review. In chapter 3, Overview of models is presented, followed by proposed methodology in chapter 4. Chapter 5 include the results and discussion part of thesis.

CHAPTER 3: OVERVIEW OF MODELS

3.1. Aspen EDR Model

Aspen Exchanger Design Rating tool (EDR) provides multiple calculation mode which are used according to need, if you want to design the heat exchanger, you will select Design Mode [45,46].

Each calculation mode is described below,

3.1.1. Design Mode

In Design Mode, program will calculate the exchanger geometry against thermal duty specified. We can also put limits on the design basis like Shell type, baffle arrangement, tube layout, tube length etc. The exchanger geometry calculated includes full exchanger details and selection of geometry depends upon either cost Optimization or Minimum Area.

3.1.2. Rating / Checking Mode

As name suggests this mode gives answer to the question “Will this exchanger do this duty?” You must specify full exchanger geometry and the process stream details. Program will give you the results in the form of ratio of actual heat transfer area to the required heat transfer area.

3.1.3. Simulation Mode

This mode gives answer to the question “What duty will this exchanger achieve?” This mode requires all process information, exchanger geometry and calculates the outlet process stream conditions and duty based on the geometry we specified.

3.1.4. Find Fouling Mode

This gives the answer to the question “what is the maximum fouling for specific thermal duty be obtained?” It requires same input as rating mode and calculates the Area Ratio by including the maximum fouling that can be deposited on either Shell Side, Tube Side, or both. Calculation modes in aspen exchanger design and rating tool are shown in [Figure 7](#).



Figure 7: Calculation Modes in Aspen Exchanger Design and Rating Tool

In this study, the rating mode is used as the complete information of heat exchanger geometry is known. First of all, the given process stream data is specified by clicking on the tab “set process data”. The properties of the crude oil and kerosene steams are specified by clicking on the tab “set properties”. Furthermore, the information about geometry of the exchanger shown in [Table 2](#) is defined in the tab “set geometry”. At the end, some construction details are defined before running the model.

Table 2: Exchanger Geometry Details Requirement

Shells	<ul style="list-style-type: none"> • Inside Diameter • Outside Diameter • Shell in Series • Shell in Parallel
Tubes	<ul style="list-style-type: none"> • Number of Tubes • Length of Tubes • Outside Diameter • Thickness of Diameter
Tube Layout	<ul style="list-style-type: none"> • Tube Passes • Tube Pitch • Tube Pattern
Baffles	<ul style="list-style-type: none"> • Baffle Spacing • Spacing at Inlet • Number of Baffles • Spacing at Outlet • Type of Baffles • Orientation of Baffles • Cut % of Baffles
Nozzles	<ul style="list-style-type: none"> • Inlet and Outlet Nominal Pipe Size • Inlet and Outlet Nominal diameter • Number of Nozzles • Flange rating • Location of Nozzles

3.2. Genetic Algorithm

3.2.1. Background

Genetic Algorithms (GA) is an evolutionary algorithm that mimics the biological evolution process. Holland presented a concept for genetic algorithms in 1975. One of the first population-based stochastic algorithms presented in history is the GA. GA was influenced by Darwin's evolutionary theory, which mimicked the survival of fitter creatures and their genes. Many researchers have used GA's to evaluate the solution of difficult problems whose objective functions lack the properties of continuity, differentiability, etc. [47,48]. It is a population-based algorithm and is based on the concepts of natural selection and genetic inheritance. Each parameter indicates a gene, and each solution represents a chromosome. A fitness function is used by GA to assess the fitness of each member in the population. The best alternatives are picked at random using a selection (– for example roulette wheel) strategy to improve bad solutions. Because the probability is related to the fitness, this operator is somewhat more certain to select the best solutions. The probability of selecting bad solutions also increases the probability of avoiding local optima. This indicates that if perfect alternatives become stuck in a local solution, they can be extracted with the help of other solutions. This procedure is repeated unless an optimal solution(s) is (are) found or maximum number of iterations or population is reached or relative difference between solutions is less than a certain limit [49–51]. [Figure 11](#) shows the flow diagram of genetic algorithm.

3.2.2. Genetic Algorithm Operators:

a. Initial Population

Genetic algorithm needs the solutions or individual in a population to be represented in the form of chromosomes. Structure of a problem and the type of genetic operators that will be used depends upon the representation scheme used. Specific alphabets are used to develop a sequence of gene that make up the chromosome. Binary digits (0 and 1) and real value numbers can constitute these specific alphabets. It has been shown that chromosomes encoded using real value numbers results in more efficient GAs and produce better solutions [52].

The following code is used while using binary GA:

where X_i is the i -th gene and r_i is a unique random number produced for each gene in the range [0,1].

$$X_i = \begin{cases} 1 & r_i < 0.5 \\ 0 & \textit{otherwise} \end{cases}$$

The equation below is used for initializing genes in the continuous GA:

$$X_i = (ub_i - lb_i) * r_i + lb_i$$

In the above equation, X_i represents i -th gene, r_i represents random number in the range [0,1] produced independently for each gene, ub_i represents i -th gene's upper bound, and lb_i represents i -th gene's lower bound [53].

b. Selection

The major source of motivation for this element of the GA algorithm is natural selection. Successive generations in GA are generated by selection of individuals from a previous generation. Selection is based on the concept that every individual has a chance or probability of being selected once or more than once, based on their fitness value, for reproduction in the next generation [54]. Assignment of probability of selection to individuals is a common step in all of these schemes. [Figure 8](#) shows the mechanism of roulette wheel in genetic algorithm. There are various methods for this assignment like roulette wheel, linear ranking and geometric ranking [55,56].

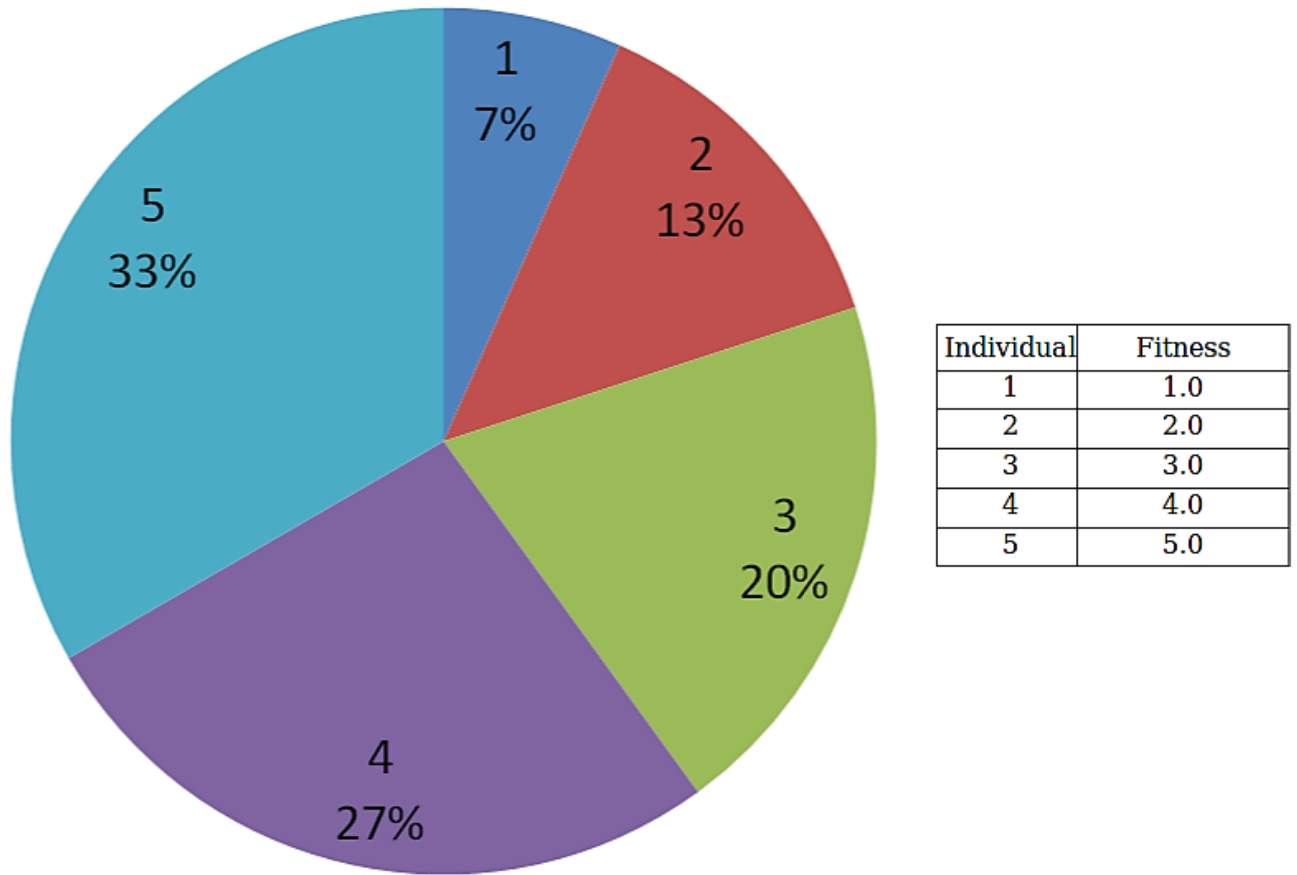


Figure 8: Mechanism of roulette wheel in genetic algorithm

c. Crossover

Crossing overtakes two individual chromosomes and transfer portion of these chromosomes between both to produce two new chromosomes. Individuals must be used to generate the new generation after being selected using a selection operator. Naturally, the chromosomes of male and female genes are joined to form a new chromosome [57]. In the GA algorithm, this is emulated by merging two solutions (parent solutions) chosen by the roulette wheel to create two new solutions (children's solutions). In the literature, there are several crossover operators approaches, two of which are depicted in Figure 9. The genes of two parent solutions are exchanged before and after a single point in a single point cross over. However, in a double-point crossover, two crossing points are present and only the chromosomes between them are exchanged [58].

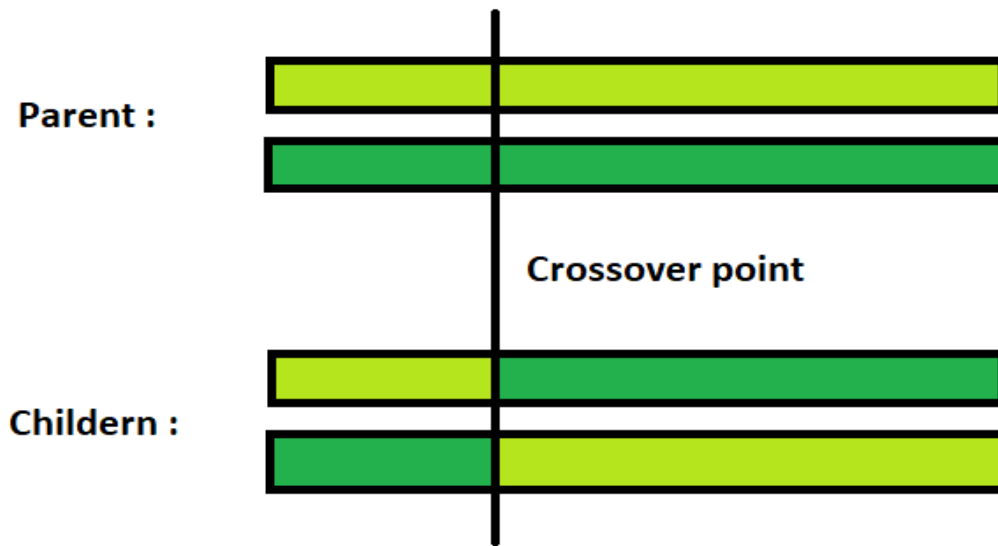


Figure 9: Single-point and double-point crossover are two prominent crossover strategies in GA.

d. Mutation

In mutation a single chromosome is altered at a single location to produce a new chromosome. It is a final evolutionary operator, in which one or more genes are changed after children solutions are created. GA has a low mutation rate because large mutation rates turn GA into a rudimentary random search. By adding another degree of unpredictability to the population, the mutation operator keeps the population diverse [59]. In the GA algorithm, this operator avoids solutions from becoming identical and increases the chances of avoiding local solutions. [Figure 10](#) depicts a conceptual illustration of this operator. After the crossover (replication) phase, minor alterations in some of the randomly chosen genes may be detected in this diagram [60].

Genetic Algorithm Mutation

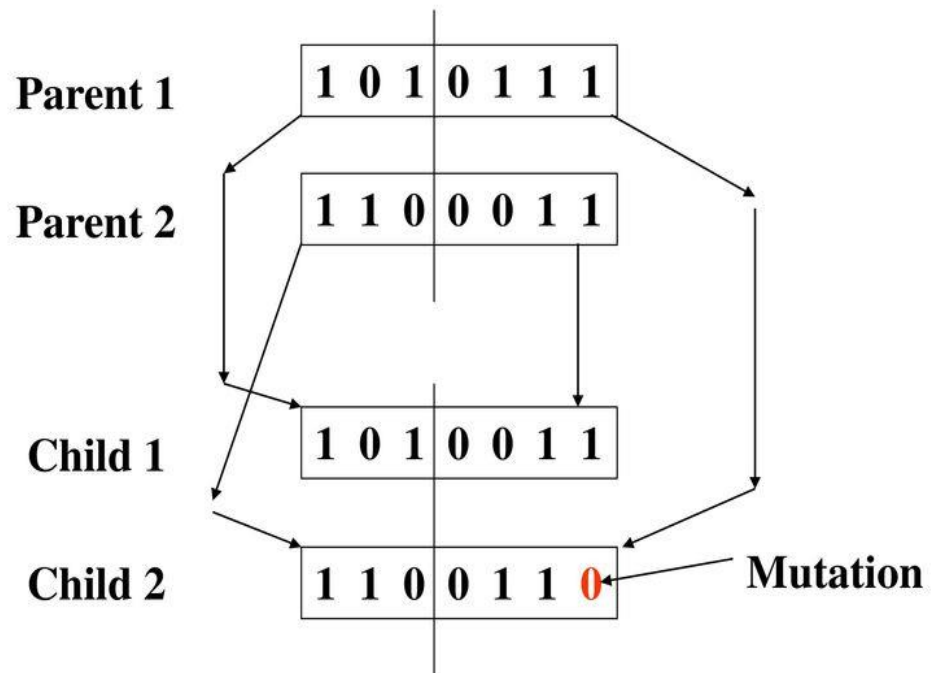


Figure 10: After the crossover phase, the mutation operator changes one or more genes in the children's solutions

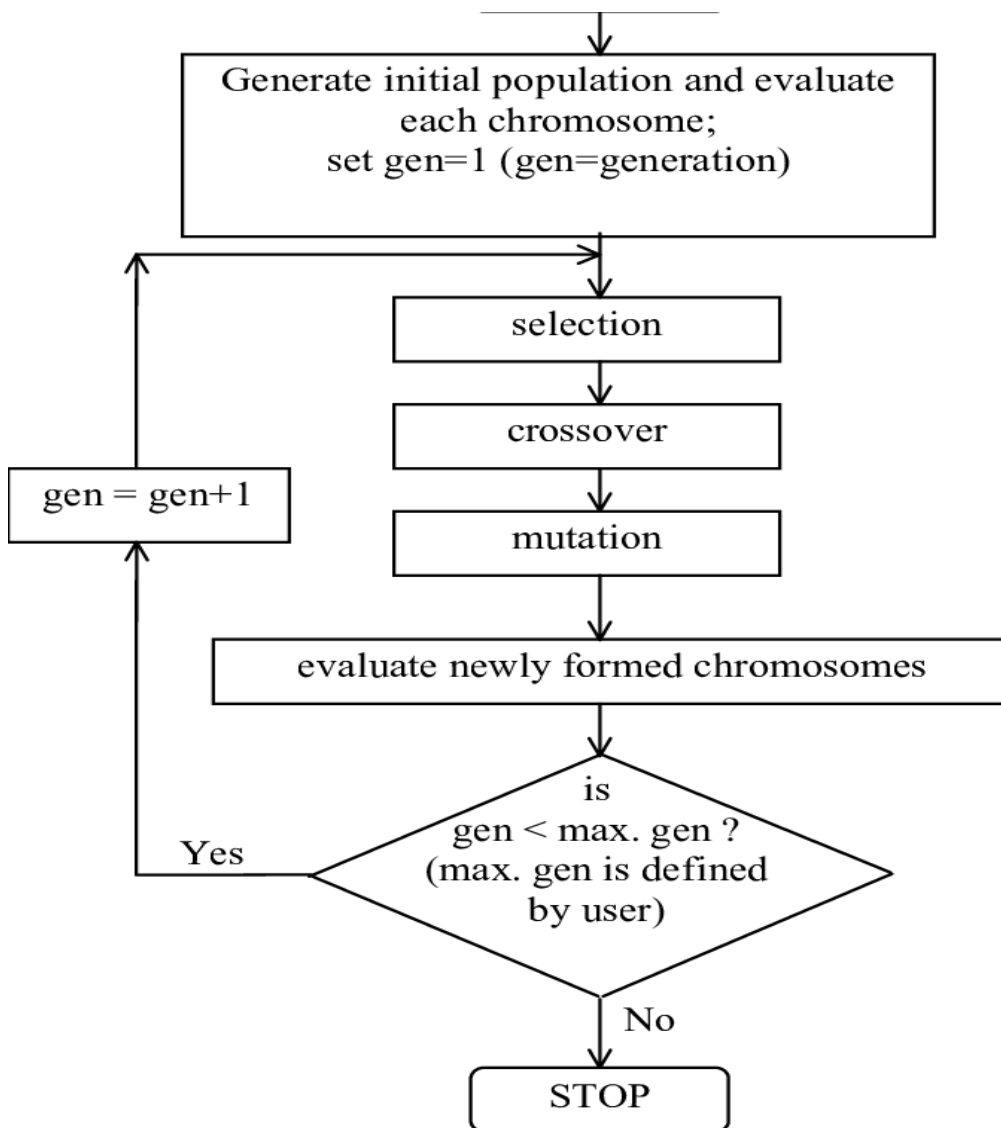


Figure 11: Flow diagram of Genetic Algorithm

3.3. Artificial Neural Network

3.3.1. Background

The concept of an artificial neural network (ANN) was first presented in the field of biology, where neural networks play a crucial role in the human body. Hebb's rule, which was established on hypotheses and findings of neurophysiologic nature, was introduced in 1949 as a first approach for training ANN. ANN are computer models based on the nervous system of live organisms. They may acquire and store knowledge (information-based) and can be described as a group of processing units depicted by artificial neurons, unified by a huge quantity of interconnections, and executed by synaptic weights vectors and matrices [61,62].

3.3.2. ANN Architecture and Training Process

Generally, an ANN comprises of input, hidden, and output layers, which are described as follows,

a. Input layer

The input layer is in charge of getting data, signals, characteristics, or assessments from the outside world. These inputs are often normalized within the bounds of activation functions. This normalization improves the numerical consistency of the network's numerical computations.

b. Hidden, intermediate, or invisible layers

The hidden layers are made up of neurons that are in charge of extracting information related to the system under investigation. These layers handle the network's internal operations.

c. Output layer

This layer, like the preceding levels, is made up of neurons and is in charge of creating and displaying the final network outputs, which are the consequence of the processing done by the neurons in the preceding layer. The major designs of ANNs may be classified into the following categories, taking into account the neuron outlook, and how they are unified and how their layers are composed: There are four types of neural networks: recurrent networks, mesh networks, single-layer, and multilayer feed forward networks [63–65]. General architecture of ANN model is shown in [Figure 12](#)

The log sigmoid is shown by equation (1)

$$f(x) = \frac{1}{1+\exp(-Y)} \text{ ----- (1)}$$

Tansigmoid transfer function is represented by equation (2) which is mostly used in the hidden layer.

$$f(x) = \frac{\exp(Y) - \exp(-Y)}{\exp(Y) + \exp(-Y)} \text{ ----- (2)}$$

Purlin is the linear transfer function which mostly uses in the output layer as represented by equation (3).

$$f(x) = Y \text{ -----(3)}$$

In the above equations, Y represents the output of the summing junction.

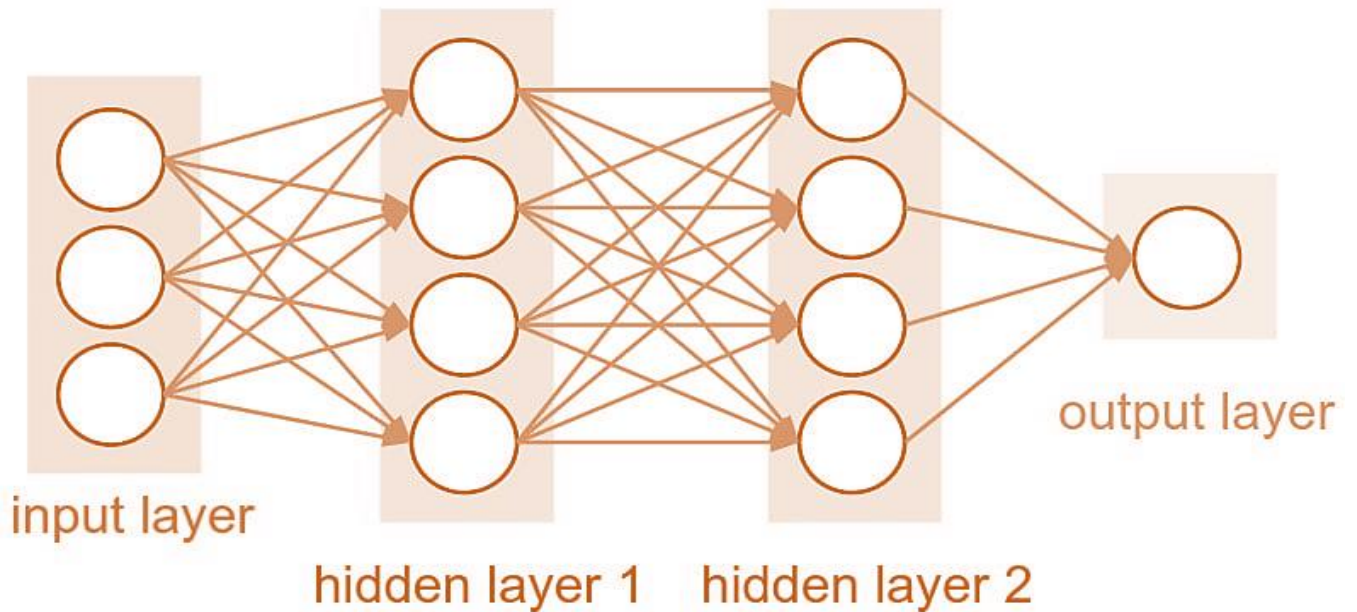


Figure 12: General architecture of ANN model.

3.4. Exergy Analysis

The second law of thermodynamics gives designers and engineers a prevailing and effective tool known as exergy analysis, which can be used to analyze heat exchanger performance. Exergy is a measure of how far a system's state deviates from that of its surroundings. It can be defined as the maximum amount of work that can be obtained from the system when it's come to equilibrium with the environment. Exergy, unlike energy, is not conserved; rather, it is destroyed by irreversibility's. Because of these irreversibility's, exergy loss during a process is proportionally related to entropy generation [66,67]. The following formulas were used to calculate exergy. In Figure 13, the stream 1 and stream 2 represent inlet and outlet for the hot stream (Kerosene) and stream 3 and stream 4 represent the inlet and outlet for the cold stream respectively. The equations 1 to 6 was used for the exergy analysis of STHE

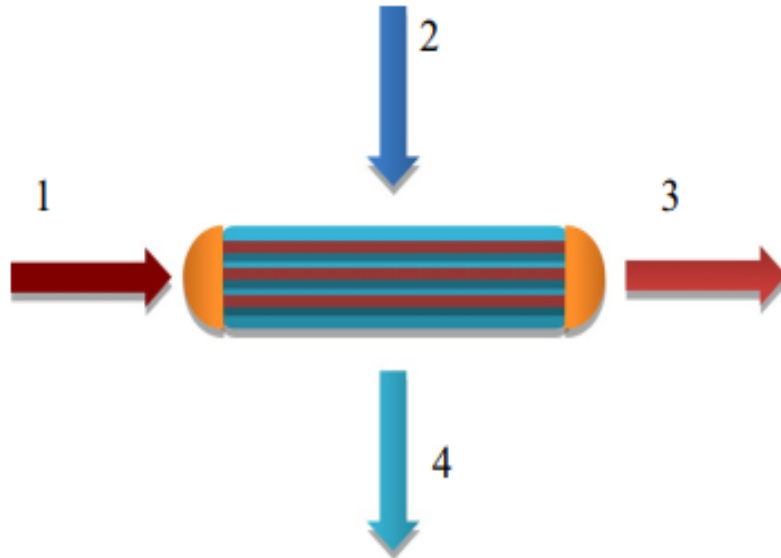


Figure 13: Schematic of Shell and tube heat exchanger

The physical exergy is calculated from enthalpy and entropy change in thermal systems as noted;

$$Ex_{ph} = (H - H_o) - T_o (S - S_o) \text{ ----- (4)}$$

Ex_{ph} represents the physical exergy of the stream, T_o shows the environmental temperature (25 oC), H and S are the enthalpy and entropy of the stream, respectively, and H_o and S_o denotes the enthalpy and entropy of the stream at environmental conditions (25 oC, 1 bar).

The equation for the exergy of destruction is as follows.

$$\text{Exergy destruction} = (\text{Ex}_1 + \text{Ex}_2) - (\text{Ex}_3 + \text{Ex}_4) \text{----- (5)}$$

Where the Ex_1 , Ex_2 , Ex_3 , and Ex_4 represents the exergy of stream 1, 2, 3, and 4, respectively.

The equation for the exergy efficiency is as follows.

$$\text{Exergy Efficiency} = \frac{(\text{Ex}_4 - \text{Ex}_2)}{(\text{Ex}_1 - \text{Ex}_3)} \text{----- (6)}$$

CHAPTER 4: METHODOLOGY

4.1. Overview of Methodology

The current work regenerated a STHE model in Aspen EDR using optimized industrial data. The optimized shell and tube heat exchanger model was then imported into Aspen HYSYS. The MATLAB and Aspen HYSYS interfaces were developed to generate a data set. Using a single objective genetic algorithm to find the optimum feed flow rate while changing the crude composition and other process conditions. Then finally Artificial intelligence system was trained on the data set to predict the optimum feed flow rate under uncertain process conditions

An ANN model was built in this study to predict the optimum mass flow rate of kerosene and crude oil under variability in crude composition and other four process variables, which are inlet temperature and pressure of crude oil and hot kerosene oil. [Figure 14](#) depicts the flow diagram of the current research work. Which consists of three major steps.

Step I: The detailed design of STHE was regenerated in Aspen EDR using optimized industrial data of STHE. The Aspen EDR model of STHE was then transferred to Aspen HYSYS.

Step II: The COM server was used to build the interface between Aspen HYSYS and MATLAB. The data set was generated by inserted the ± 1 , ± 2 , ± 3 , ± 4 and ± 5 variations in the crude oil composition and inlet temperature and pressure of crude and hot kerosene oil. Using a single objective genetic algorithm, the optimum mass flow rate was determined for each variation. The objective function was to minimize the outlet temperature of hot kerosene oil, to reduce energy consumption.

Step III: The 400 data points were produced, with 70 percent used for training and the residual data set split evenly for validation and testing of the ANN model. [Table 3](#) shows the ten samples' data generated for the process variables.

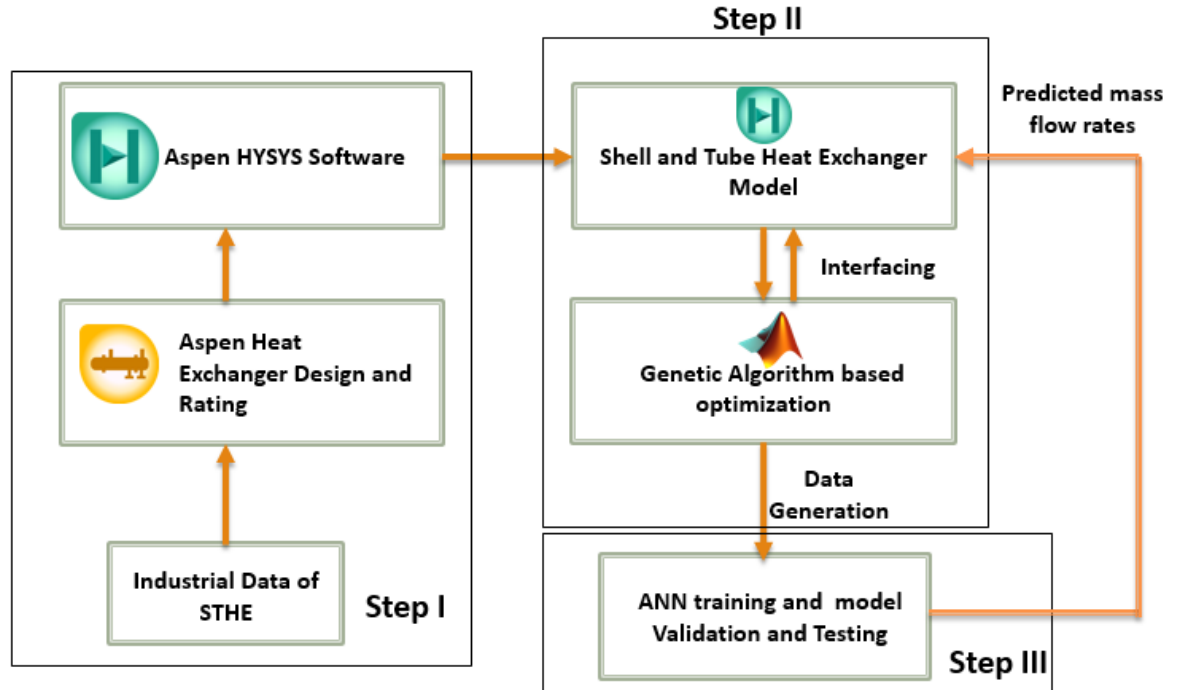


Figure 14: Flow diagram of the present research work

4.2. Process Data

Figure 15 represents the STHE model. The heat exchanger was used to transfer heat between hot kerosene and cold crude oil. The crude oil was located on the tube side, while the hot kerosene was located on the shell side. The local Pakistani crude oil i.e., kunnar blend was used for this study. The hot kerosene oil coming from the crude distillation unit (CDU) has a mass flow of 68004 lb/hr. The inlet temperature and pressure for hot kerosene oil were 448 °F and 226 psig. The crude oil has a mass flow of 222586 lb/hr. The inlet temperature and pressure for the cold crude oil were 115 °F and 202 psig, respectively. The allowable pressure drop of tube and shell side of STHE was 14 and 7 psi, respectively. The detailed geometrical design parameter of the present STHE can be seen in Table 3.

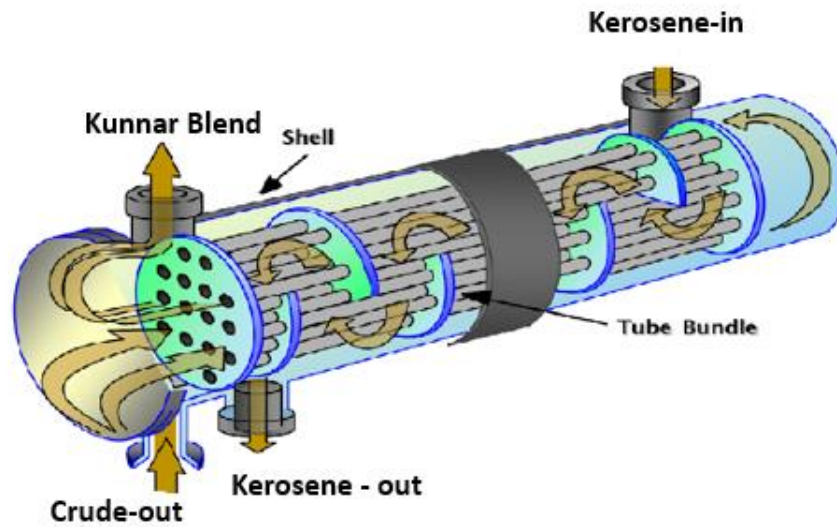


Figure 15: Shell and tube heat Exchanger model

Table 3: Design parameters of STHE

Parameter	Value	Parameter	Value
Number of tubes	448	Baffles type	Single-segmental
Number of tubes passes	6	Baffle cut	25%
Tube Length (ft.)	22	Baffle spacing (inch)	8
Tube outside diameter (inch)	1.05	Allowable pressure drops (psi) Shell side	7
Number of shell passes	2	Allowable pressure drops (psi) tube side	14
Shell Inside diameter (inch)	32.2	Fouling Factor (hr. ft. °F/Btu) on shell side	0.0033
Pitch	triangular	Fouling Factor (hr. ft. °F/Btu) on tube side	0.0045
Number of baffles	43	Area (ft ²)	1329

4.3. Aspen EDR Model Development

4.3.1. Simple Heat Exchanger Models

In this study STHE model was first simulated in Aspen HYSYS using the steps shown in Figures 16, 17, and 18.

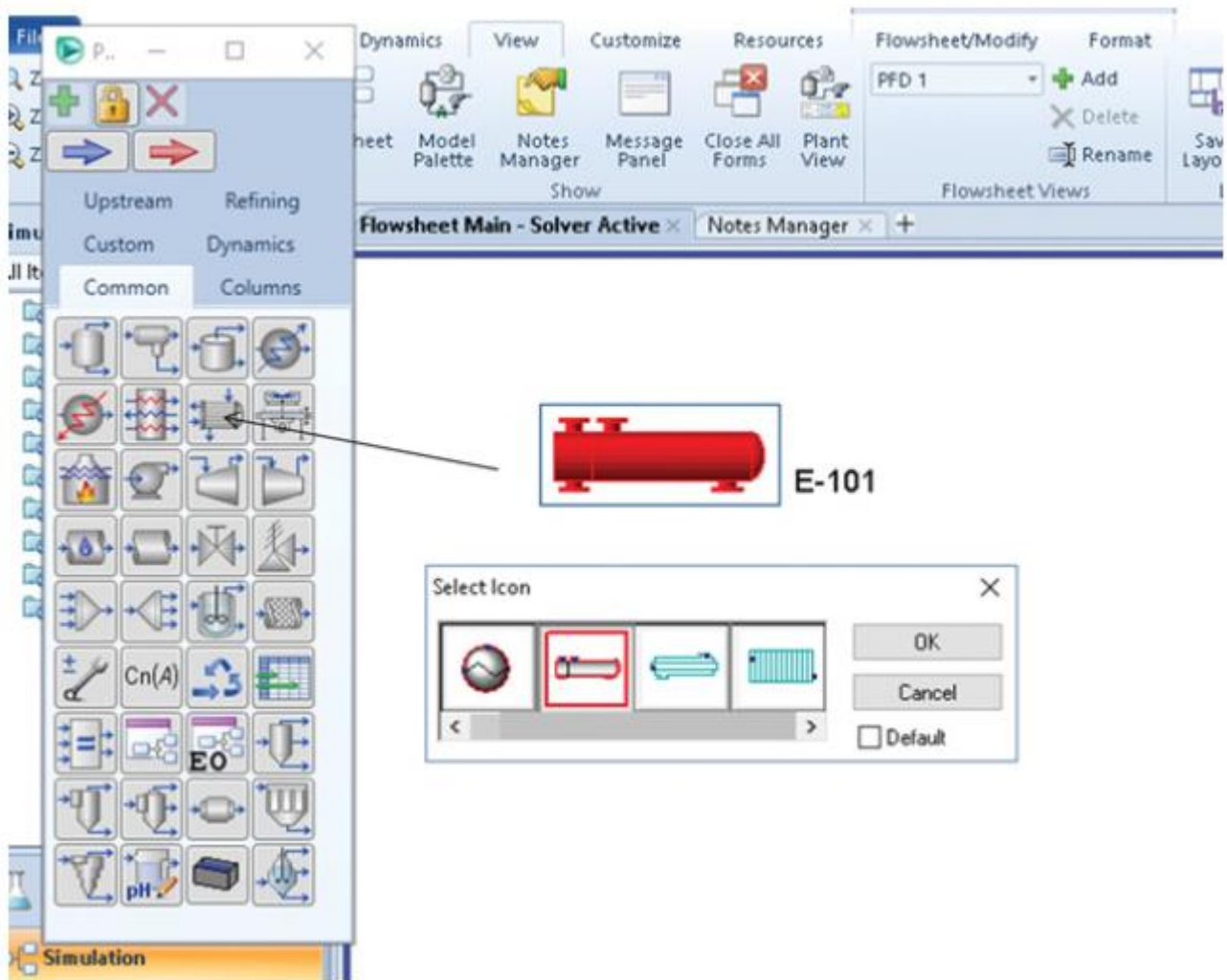


Figure 16: Selection of STHE Model in Aspen HYSYS

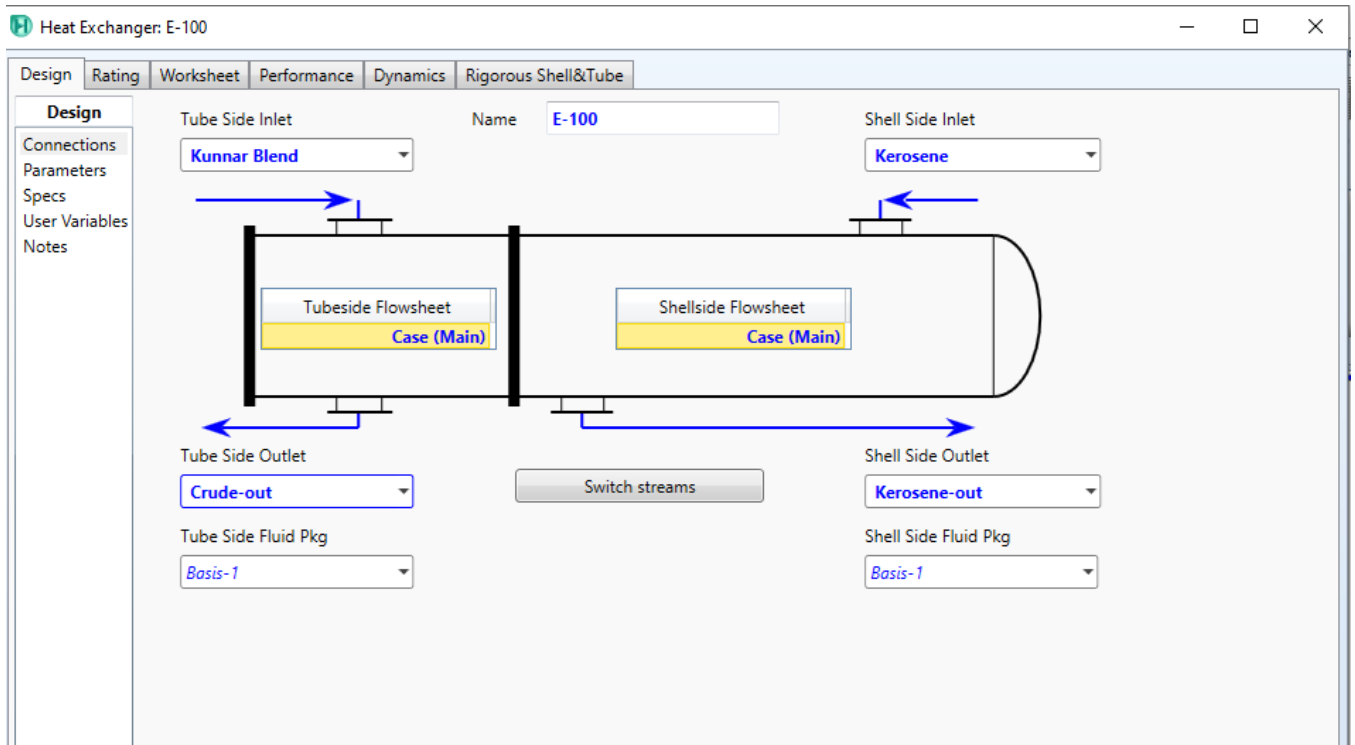


Figure 17: Connections of stream in STHE model

Name	Kunnar Blend	Crude-out	Kerosene	Kerosene-out
Vapour	0.0000	0.0000	0.0000	0.0000
Temperature [C]	27.78	62.50	160.0	64.94
Pressure [kPa]	1420	1362	1214	1208
Molar Flow [kgmole/h]	505.3	505.3	203.6	203.6
Mass Flow [kg/h]	7.212e+004	7.212e+004	2.203e+004	2.203e+004
Std Ideal Liq Vol Flow [m3/h]	91.08	91.08	29.57	29.57
Molar Enthalpy [kJ/kgmole]	-3.090e+005	-2.990e+005	-2.031e+005	-2.280e+005
Molar Entropy [kJ/kgmole-C]	159.5	191.0	168.4	103.8
Heat Flow [kJ/h]	-1.561e+008	-1.511e+008	-4.136e+007	-4.642e+007

Figure 18: Entering input parameter using worksheet page

4.3.2. Detail Model Development

The rigorous rating model of STHE was developed in Aspen EDR using the following step

- Open Aspen EDR and click on the import tab in the File menu to import the previous Aspen HYSY model to Aspen EDR.
- Select the Rating mode from the home menu
- Click on the Set process data in the home menu to specify the inputs variables for the STHE model as shown in [Figure 19](#).
- Click on the Set Geometry tab in the home menu to specify the geometrical information for STHE model as given in the [Table 3](#). The geometrical information was shown in [Figure 20](#).
- Finally Set Construction specification and run the simulation

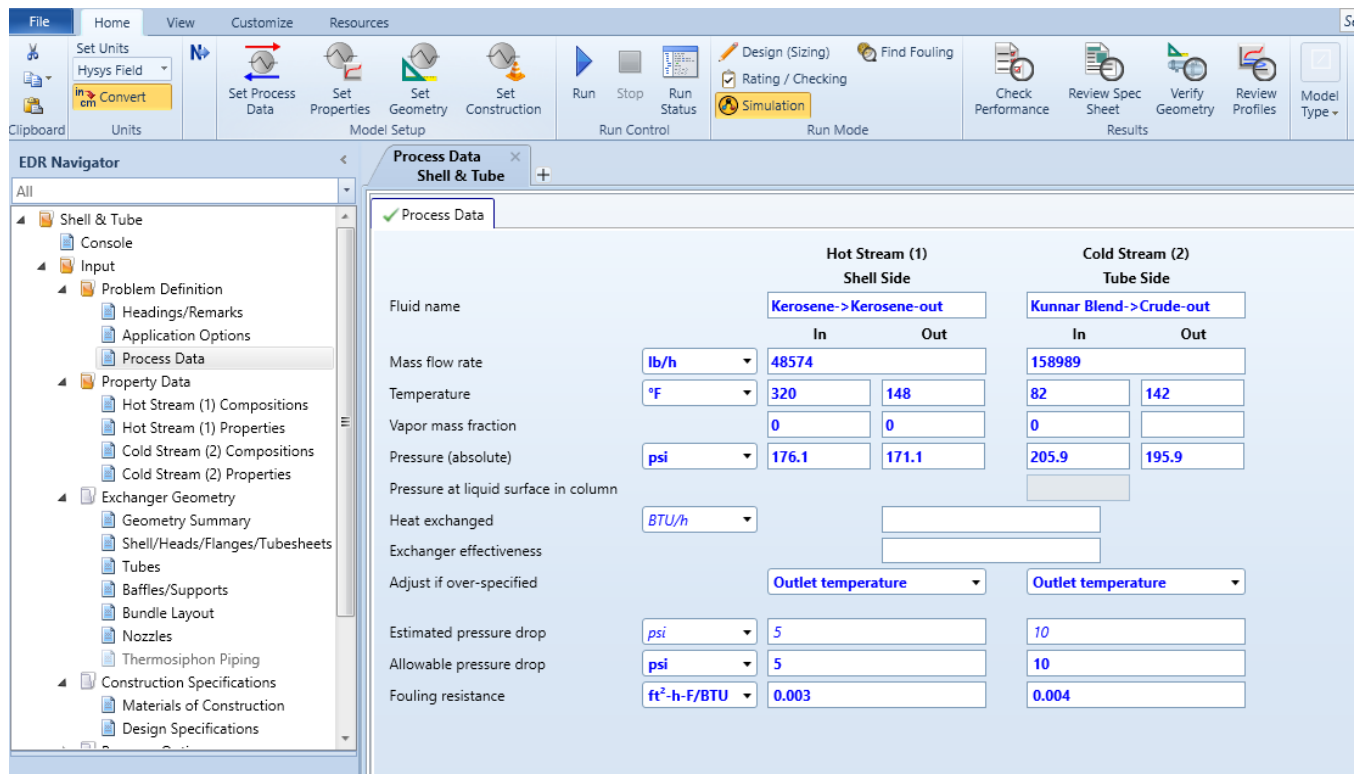


Figure 19: Entering inputs for the STHE model

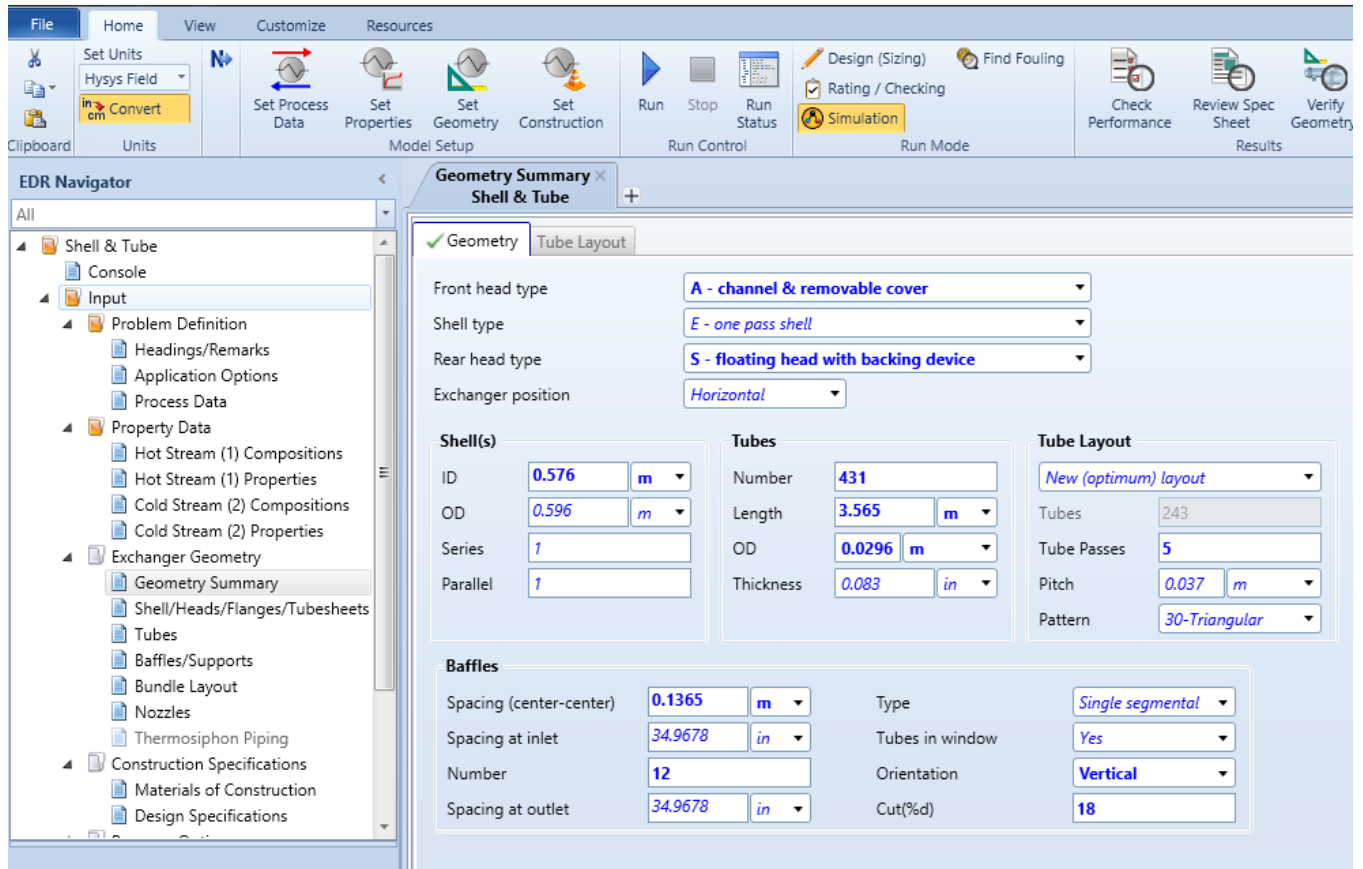


Figure 20: Entering geometrical information for STHE model in Aspen EDR

4.4. Aspen HYSYS and MATLAB Interfacing

The detail Aspen EDR model of STHE was first imported in Aspen HYSYS. The five process variables i.e., crude composition, inlet crude stream temperature, inlet crude stream pressure, inlet kerosene stream pressure and inlet kerosene stream temperature were selected as uncertain variables. The five uncertain process variables and objective variable (crude outlet temperature) were imported to spreadsheet inside Aspen HYSYS. Then interface between the spreadsheet of Aspen HYSYS and MATLAB software was developed using COM server as shown in [Figure 21](#).

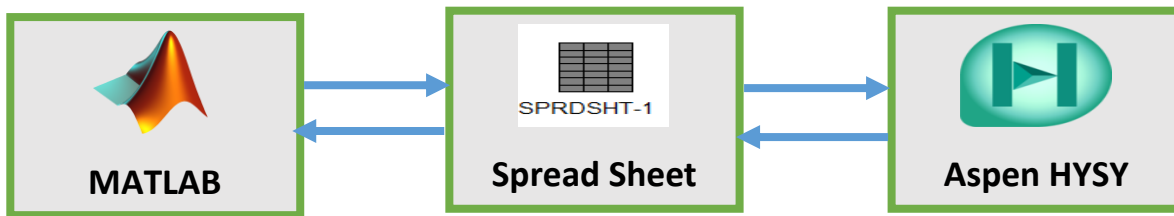


Figure 21: MATLAB and Aspen HYSY interfacing

4.5. Single objective Genetic algorithm for optimization

In this study single objective genetic algorithm was used to optimize the inlet streams mass flow rate under uncertainty in the selected five process variables. The objective function for the GA was to minimize the crude outlet temperature. The inlet crude oil and inlet kerosene stream mass flow rate were selected as manipulating variables for GA. The inbuilt function i.e., “ga” command of MATLAB software was used for the implementation of single objective genetic algorithm. The population size and number of generations were 20 and 5 respectively. The Following lines describes the workflow for genetic algorithm.

- First, the uncertainty in the selected process variables was brought.
- Then the genetic algorithm generates the initial populations of size 20
- Each chromosome in the population was put in the Aspen HYSY software to evaluate the objective function i.e., crude outlet temperature
- When one generation is completed the population for the next generation was selected using GA operator i.e., selection, crossover and mutations.
- This process was continued up to 5 generation
- After the completions of number of generations, the mass flow rate of crude oil and kerosene stream that gives the minimum outlet temperature of crude stream was selected as a best solution.

4.6. Data generation

Using Aspen HYSYS and MATLAB interfacing the data was generated to train Feed Forward Neural network (ANN). A total of 400 data points were generated. The data was generated using the 5 % uncertainty in the process variables which include the crude composition, crude temperature, crude pressure, and kerosene temperature and kerosene pressure. Table 4 shows ten data samples of generated data for four process variables. The first row of data points were generated with -5 percent variation, the second row with -4 percent variation, the third row with -3 percent variation and so on until the last row with +1 percent variation.

Table 4: Ten Data sample of generated data

Datasets	Crude inlet Temperature (°C)	Crude inlet Pressure (Kpa)	Kerosene inlet Temperature (°C)	Kerosene inlet Pressure (Kpa)
Dataset 1	36.94	1888.07	212.80	1614.81
Dataset 2	35.47	1812.55	204.29	1550.21
Dataset 3	34.40	1758.17	198.16	1503.71
Dataset 4	33.71	1723.01	194.20	1473.63
Dataset 5	33.38	1705.78	192.25	1458.90
Dataset 6	33.71	1722.84	194.18	1473.48
Dataset 7	34.39	1757.29	198.06	1502.95
Dataset 8	35.42	1810.01	204.00	1548.04
Dataset 9	36.83	1882.41	212.16	1609.97

4.7. Artificial neural network (ANN) model training and validation

ANN model was trained using the data generated from Aspen HYSYS and MATLAB interfacing. A total of 400 data points were generated, with 70% used for training, 15% for validation, and 15% for testing the ANN model. Multi-output Feed forward multilayer neural network was trained with the Levenberg-Marquardt (trainlm) training algorithm. The crude stream composition, inlet crude stream temperature, inlet crude stream pressure, kerosene stream inlet temperature and kerosene stream inlet pressure were considered as an input to ANN model. The mass flow rates of hot kerosene oil and cold crude oil were considered as an output of the ANN model. The objective function for GA was the root mean square error (RMSE) for the three outputs of the ANN model. Both generation and population of 50 was selected. The optimum architecture of ANN consists of 3 hidden layers. The number of neurons in layers 1, 2 and 3 were 19, 18 and 20, respectively as shown in Figure 22. The optimum ANN model has the RMSE of 0.4316 and 0.0461 for the mass flow rate of crude oil and kerosene oil respectively. The tansig and purlin activation function was used in the hidden layer and output layer, respectively. The Figure 23 shows the ANN model based predicted values of mass flow of crude oil and kerosene oil vs. the target values. The trained ANN model has a high correlation coefficient of 0.999 which make it suitable for industrial applications.

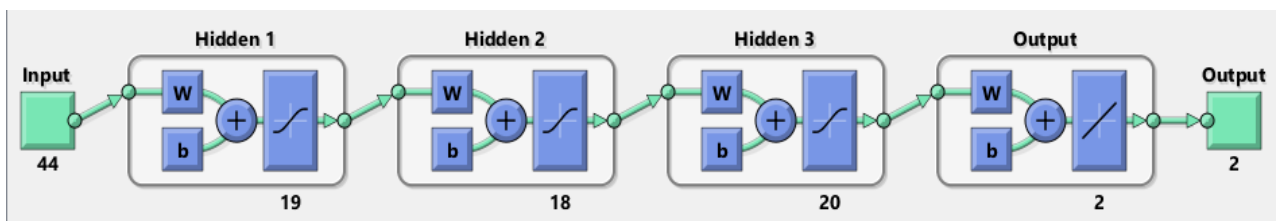


Figure 21: Proposed ANN model Architecture

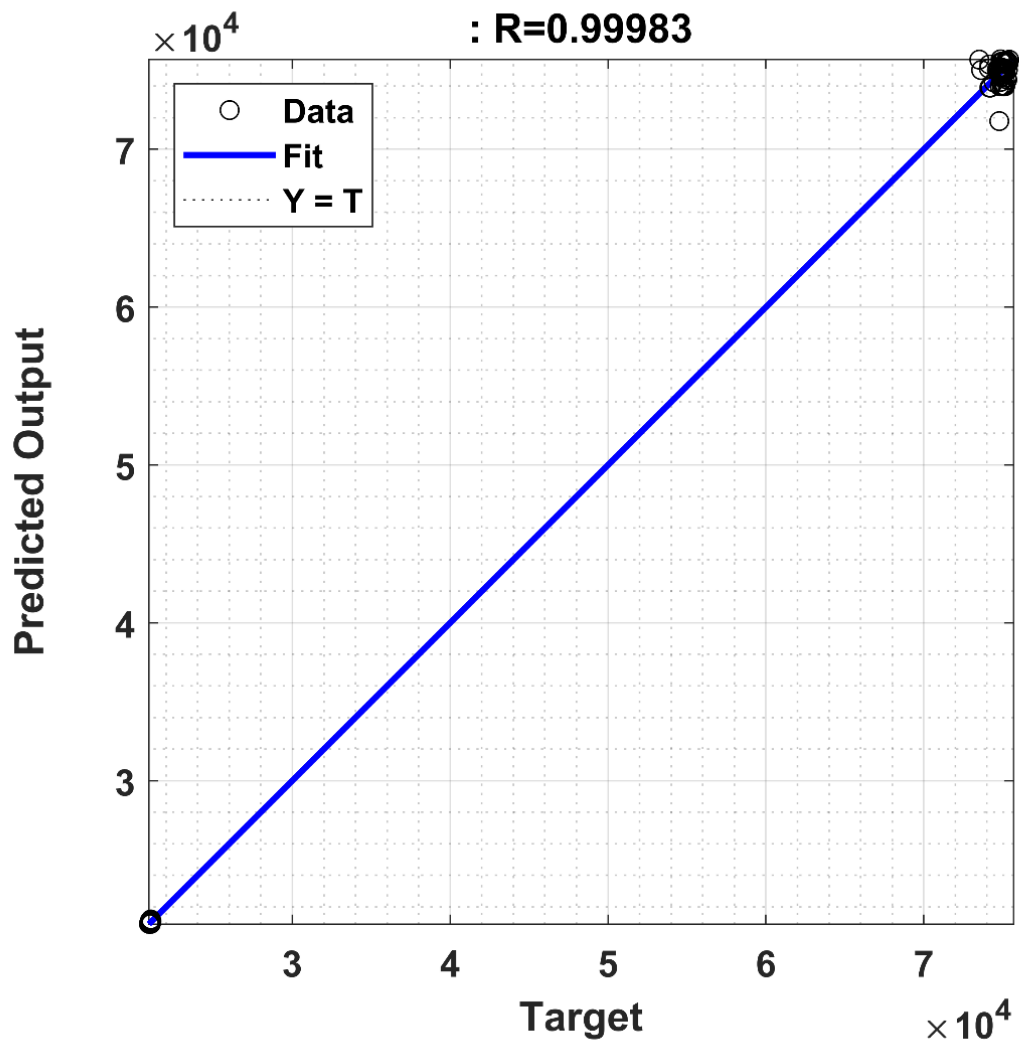


Figure 22: Actual vs. predicted value based on ANN model

CHAPTER 5: RESULTS AND DISCUSSION

5.1. Optimization through Genetic Algorithm

The inlet crude composition, crude stream inlet temperature, crude stream inlet pressure, kerosene inlet temperature, and kerosene inlet pressure were all subjected to 5% variations. The goal of using a single objective GA was to find the optimum mass flow rates of crude oil and kerosene oil entering the STHE under each variation while minimizing kerosene outlet temperature. The upper and lower bounds for mass flow rates were determined by a 5% variation in the initial mass flow rates of cold crude oil and hot kerosene oil streams. The number of generations and population size of 20 and 5 were chosen for the genetic algorithm respectively. [Table 5](#) compares the results of the straight run and the genetic algorithm for 19 data samples. Straight run (SR) in this study refer to the simulation of the STHE model under uncertainty in the process variables without optimizing the crude oil and kerosene oil mass flow rates.

[Table 5](#) shows that the genetic algorithm outperforms the straight run. The genetic algorithm results show higher effectiveness and lower hot kerosene outlet temperature than the straight run results. The following lines describe the workflow for the genetic algorithm. Firstly, the genetic algorithm generates the initial populations of size 20. Each chromosome in the population was put in the Aspen HYSYS software to evaluate the objective function i.e., crude outlet temperature. When one generation has completed the population for the next generation was selected using GA operator i.e., selection, crossover, and mutations. This process was continued up to 5 generations. After the completion of a number of generations, the mass flow rate of crude oil and kerosene stream that gives the minimum outlet temperature of the crude stream was selected as the best solution

Table 5: Comparison between straight run and GA

No. of samples	SR			GA		
	Kerosene Outlet Temp	Crude Outlet Temp	Effectiveness	Kerosene Outlet Temp	Crude Outlet Temp	Effectiveness
Case1	82.64	79.34	0.7205	79.09	76.33	0.741
Case2	80.09	76.82	0.7209	77.28	74.48	0.738
Case3	90.38	86.98	0.7191	87.08	84.13	0.737
Case4	77.66	74.40	0.7213	74.83	72.00	0.739
Case5	78.46	75.18	0.7211	75.63	73.00	0.738
Case6	80.07	76.78	0.7209	77.29	74.48	0.737
Case7	90.38	86.98	0.7191	86.69	83.80	0.739
Case8	88.56	82.07	0.7049	85.64	79.88	0.721
Case9	82.67	79.34	0.7203	79.32	76.50	0.74
Case10	78.46	75.18	0.7211	75.46	72.80	0.739

5.2. Prediction through ANN

Table 6 and Table 7 shows the comparison between the straight run (SR), genetic algorithm (GA) and ANN based prediction of the hot kerosene oil outlet temperature and effectiveness of STHE respectively. A total of 400 data points were generated, with 70% used for training, 15% for validation, and 15% for testing the ANN model. Multi-output Feed forward multilayer neural network was trained with the Levenberg-Marquardt (trainlm) training algorithm. The number of hidden layers and number of neurons in the hidden layer was selected using multi-objective genetic algorithm approach. The optimum architecture of ANN consists of 3 hidden layers. The number of neurons in layers 1, 2 and 3 were 19, 18 and 20, respectively. The tansig and purlin activation function was used in the hidden layer and output layer, respectively. The trained ANN model has a high correlation coefficient of 0.999 which make it suitable for industrial applications.

Figure 24 compares the Straight (SR), ANN, and Genetic algorithms for the average value of kerosene outlet temperature. The prediction based on the ANN model and the genetic algorithm is nearly identical. A similar trend was observed in the case of effectiveness as shown in Figure 25. In the case of effectiveness, the difference between the average value predicted by GA and ANN model was very low. The variation of kerosene outlet temperature and effectiveness over 19 data samples were shown in Figure 26 and Figure 27, respectively. It was observed that the ANN model exhibits the same trend as the GA. As a result of the high correlation coefficient and robustness of the ANN model, it is suitable for real-time industrial applications, to reduce energy consumption and increase the equipment life by enhancing the effectiveness of heat exchanger.

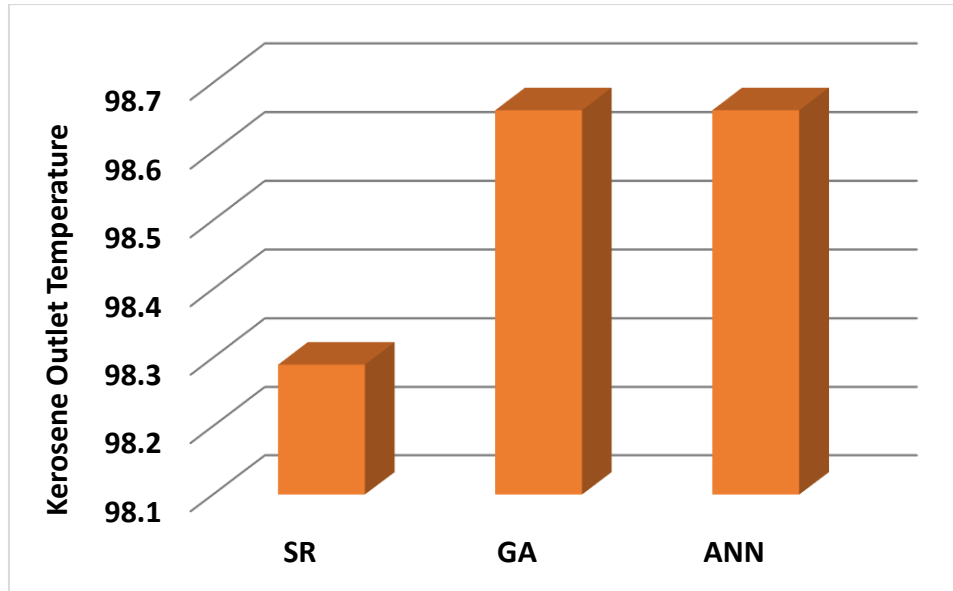


Figure 23: Average Outlet temperature value

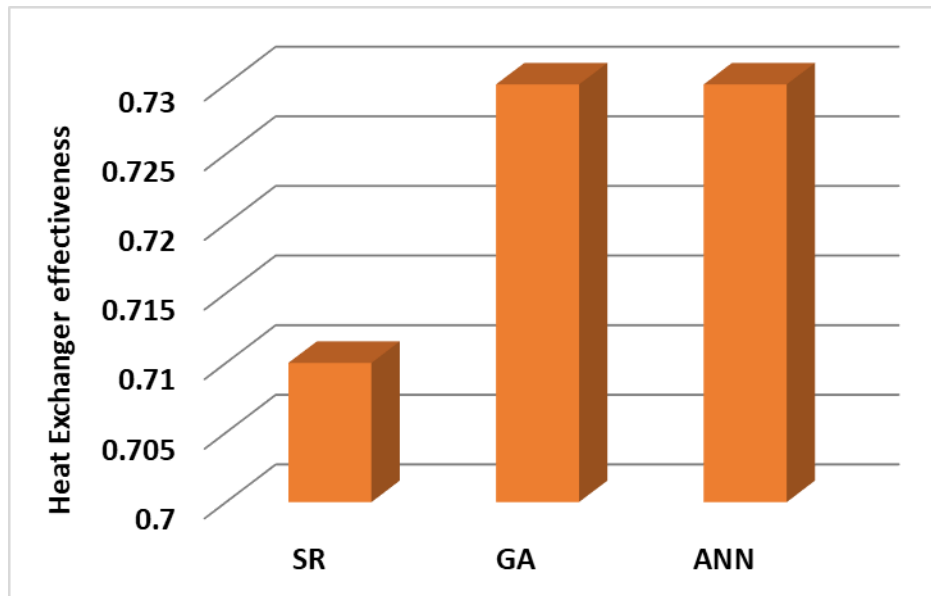


Figure 24: Average STHE effectiveness

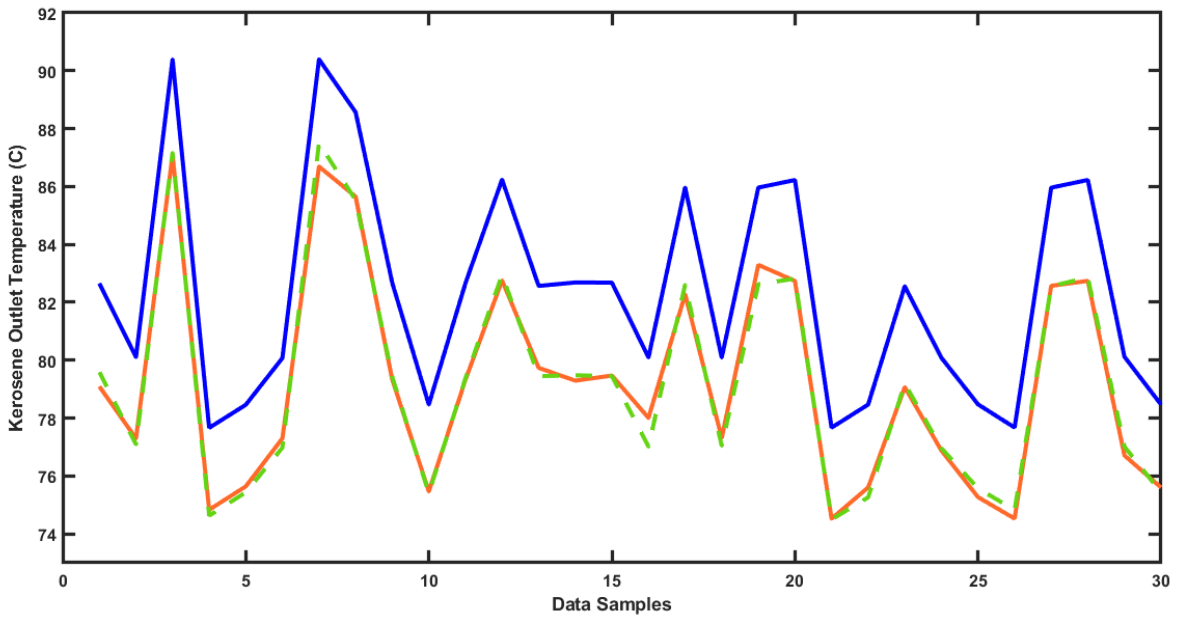


Figure 25: Comparison of Kerosene outlet temperature obtained through SR, GA, and ANN models

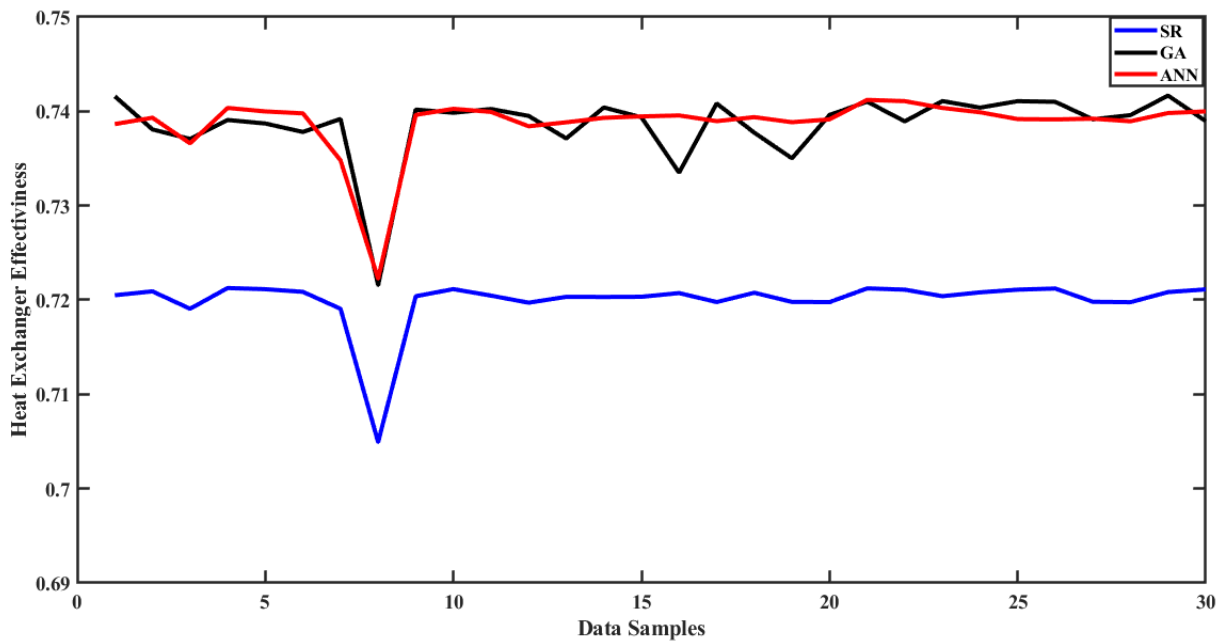


Figure 26: Comparison of STHE effectiveness obtained through SR, GA, and ANN models

Table 6: Comparison between SR, GA and ANN for kerosene outlet temperature

Number of samples	Kerosene Outlet Temperature (°C)			Crude Outlet Temperature (°C)		
	SR Temperature	GA Temperature	ANN Temperature	SR Temperature	GA Temperature	ANN Temperature
Case1	82.642	79.086	79.576	79.338	76.328	76.832
Case2	80.094	77.28	77.084	76.818	74.48	74.382
Case3	90.384	87.08	87.164	86.982	84.126	84.504
Case4	77.658	74.83	74.62	74.396	72.002	71.946
Case5	78.456	75.628	75.432	75.18	72.996	72.73
Case6	80.066	77.294	76.972	76.776	74.48	74.256
Case7	90.384	86.688	87.486	86.982	83.804	84.882
Case8	88.564	85.638	85.526	82.068	79.884	79.758
Case9	82.67	79.324	79.422	79.338	76.496	76.622
Case10	78.456	75.46	75.39	75.18	72.8	72.702

Table 7: Comparison between SR, GA, and ANN-based prediction of STHE effectiveness

Number of samples	Straight run effectiveness	GA effectiveness	ANN effectiveness
Case1	0.7205	0.7416	0.7386
Case2	0.7209	0.7381	0.7393
Case3	0.7191	0.7371	0.7366
Case4	0.7213	0.7391	0.7404
Case5	0.7211	0.7387	0.7399
Case6	0.7209	0.7378	0.7397
Case7	0.7191	0.7392	0.7348
Case8	0.7049	0.7216	0.7222
Case9	0.7203	0.7402	0.7396
Case10	0.7211	0.7398	0.7402

5.3. Exergy Analysis

The exergy analysis of the STHE is performed for the SR, GA, and ANN models. In the case of SR, exergy loss and efficiency were calculated by incorporating the artificial uncertainty in crude composition and process parameters while keeping the mass flowrates of crude and kerosene oil constant. A similar strategy was adopted for the exergy analysis of GA but in this case, the mass flowrates of crude and kerosene oil were optimized using single-objective GA. Likewise, in the case of ANN, the exergy loss and efficiency were estimated by inserting the mass flowrates of crude and kerosene oil predicted by ANN into the Aspen HYSYS model of STHE.

The enthalpy and entropy values of the crude and kerosene inlet and outlet streams are shown in [Tables 8 and 9](#), respectively. These values were taken from Aspen HYSYS model of STHE to calculate the physical exergy using equation 4. Furthermore, [Figures 28](#) depicts the exergy losses for the SR, GA, and ANN models for the STHE. The exergy loss or destruction was calculated using equation 5. The maximum average exergy losses for SR, GA, and ANN models were 23 kW, 21.3 kW, and 17 KW, respectively. [Figures 29](#) shows the exergy efficiency for all the three models (SR, GA, and ANN) for the STHE. The exergy efficiency of all the models was calculated using equation 6. The maximum average exergy efficiency for SR, GA, and ANN models were 98.2, 98.65, and 98.66, respectively.

Overall, it can be observed that the results are consistent with the exergy efficiency values, as the rise in efficiency is due to reduced irreversibilities. In comparison to the SR, the GA and ANN model showed a high exergy efficiency and lower exergy losses. Moreover, it was observed that the exergy loss, exergy efficiency, and effectiveness estimated by GA and ANN are almost identical. The high exergy efficiency means that there is little irreversibility in the process, which means that less energy is wasted, and that the equipment life is extended.

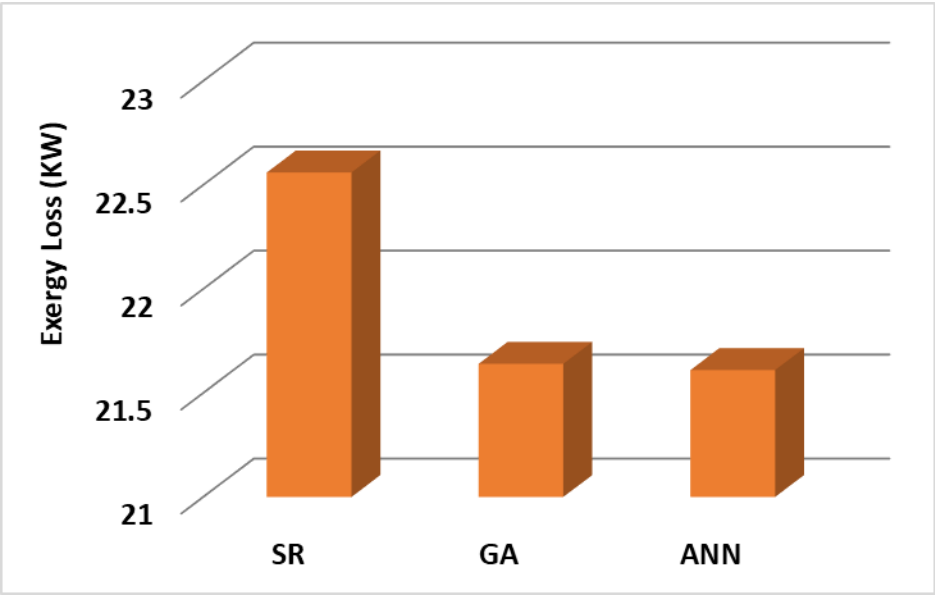


Figure 27: Average Exergy loss comparison between ANN and straight run

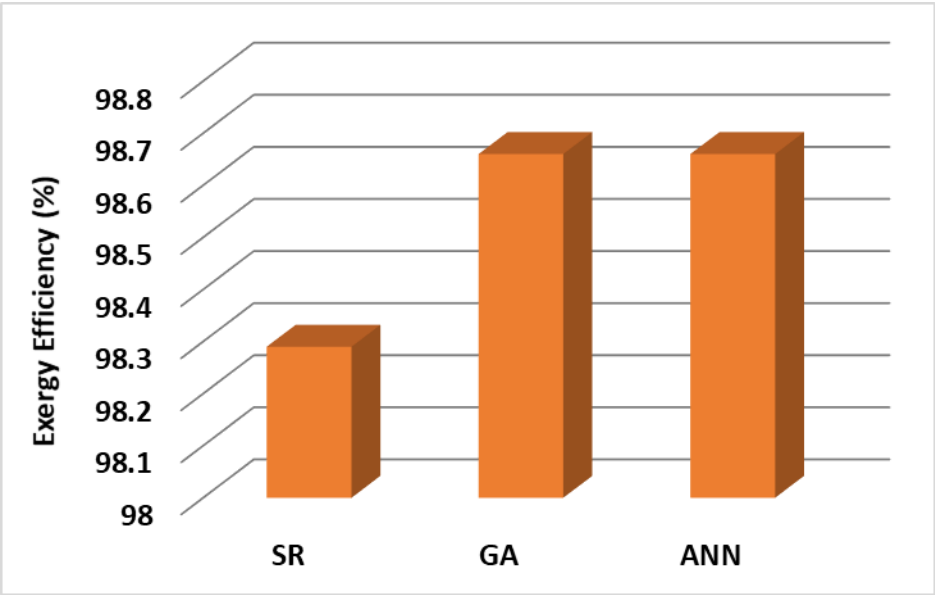


Figure 28: Exergy Efficiency predicted by the straight run and ANN model

Table 8: Enthalpy of the inlet and outlet streams of STHE

			SR						GA						ANN													
Crude Inlet Enthalpy	Crude Outlet Enthalpy	3038	2950	2680	2696	2631	2711	2978	2977	2973	2696	2706	2973	2951	2955	2660	2680	2968	2973	2951	3038	2956	2680	2975	3038	2955	2680	2974
3040	2955	3040	2696	2696	2631	2711	2978	2977	2973	2696	2706	2973	2951	2955	2660	2680	2968	2973	2951	3038	2960	2696	2711	2979	3040	2960	2696	2980
3032	2934	3032	2631	2631	2631	2711	2978	2977	2973	2696	2706	2973	2951	2955	2660	2680	2968	2973	2951	3032	2940	2631	2711	2958	3032	2939	2631	2958
3042	2960	3042	2711	2711	2711	2711	2978	2977	2973	2696	2706	2978	2977	2973	2660	2680	2968	2973	2951	3042	2965	2711	2984	3042	2965	2711	2985	
3041	2959	3041	2706	2706	2706	2706	2977	2977	2973	2706	2706	2977	2977	2973	2660	2680	2968	2973	2951	3041	2963	2706	2983	3041	2964	2706	2983	
3040	2955	3040	2696	2696	2696	2696	2973	2973	2973	2696	2696	2973	2951	2955	2660	2680	2968	2973	2951	3040	2960	2696	2979	3040	2961	2696	2980	
3032	2934	3032	2631	2631	2631	2631	2951	2951	2951	2631	2631	2951	2951	2955	2660	2680	2968	2951	2951	3032	2941	2631	2959	3032	2938	2631	2957	
3027	2937	3027	2660	2660	2660	2660	2955	2955	2955	2660	2660	2955	2955	2955	2660	2680	2968	2955	2955	3027	2941	2660	2961	3027	2942	2660	2961	
3038	2950	3038	2680	2680	2680	2680	2968	2968	2968	2680	2680	2968	2968	2968	2680	2680	2968	2968	2968	3038	2956	2680	2975	3038	2956	2680	2975	
3042	2959	3042	2706	2706	2706	2706	2977	2977	2977	2706	2706	2977	2977	2977	2706	2706	2977	2977	2977	3042	2964	2706	2983	3041	2964	2706	2983	

Table 9: Entropy of the inlet and outlet streams of STHE

			SR			GA			ANN											
Crude Inlet Entropy	Crude Outlet Entropy	Crude Inlet Entropy	Kerosene Outlet Entropy	Kerosene Inlet Entropy	Crude Outlet Entropy	Crude Inlet Entropy	Kerosene Outlet Entropy	Kerosene Inlet Entropy	Crude Outlet Entropy	Crude Inlet Entropy	Kerosene Outlet Entropy	Kerosene Inlet Entropy								
1.54	1.82	1.82	2.06	2.06	1.29	1.29	1.54	1.54	1.81	1.81	1.54	1.54	1.27	1.27	1.81	1.81	2.06	2.06	1.27	1.27
1.54	1.81	1.81	2.02	2.02	1.27	1.27	1.54	1.54	1.79	1.79	1.54	1.54	1.26	1.26	1.79	1.79	2.02	2.02	1.26	1.26
1.57	1.88	1.88	2.17	2.17	1.34	1.34	1.57	1.57	1.85	1.85	1.57	1.57	1.32	1.32	1.86	1.86	2.17	2.17	1.32	1.32
1.53	1.79	1.79	1.99	1.99	1.26	1.26	1.53	1.53	1.78	1.78	1.53	1.53	1.25	1.25	1.78	1.78	1.99	1.99	1.23	1.23
1.53	1.79	1.79	1.99	1.99	1.26	1.26	1.53	1.53	1.78	1.78	1.53	1.53	1.25	1.25	1.78	1.78	1.99	1.99	1.25	1.25
1.54	1.81	1.81	2.02	2.02	1.27	1.27	1.54	1.54	1.79	1.79	1.54	1.54	1.26	1.26	1.79	1.79	2.02	2.02	1.26	1.26
1.57	1.88	1.88	2.17	2.17	1.34	1.34	1.57	1.57	1.85	1.85	1.57	1.57	1.32	1.32	1.86	1.86	2.17	2.17	1.32	1.32
1.74	2.02	2.02	2.1	2.1	1.33	1.33	1.74	1.74	2	2	1.74	1.74	1.32	1.32	2	2	2.1	2.1	1.32	1.32
1.54	1.82	1.82	2.06	2.06	1.29	1.29	1.54	1.54	1.81	1.81	1.54	1.54	1.27	1.27	1.81	1.81	2.06	2.06	1.27	1.27
1.53	1.79	1.79	1.99	1.99	1.26	1.26	1.53	1.53	1.78	1.78	1.53	1.53	1.25	1.25	1.78	1.78	1.99	1.99	1.25	1.25

5.5. Graphical User Interface (GUI)

Figure 30 depicts an easy-to-use graphical user interface created in MATLAB. When the inlet process stream conditions are uncertain, the GUI is used to predict the mass flow rate of the inlet streams using the proposed ANN model. The GUI interface was created with the aim of providing an easy-to-use interface to the end user. The following are instructions about how to get results from a GUI.

- Put the input data of four process variables i.e., inlet streams temperature and pressure into the input data panel
- Load the composition of the crude oil from the excel file using the ‘Load.xls’
- Press the ‘Run’ button to see the results in the Result panel
- Use the ‘Reset button’ to clear all the data

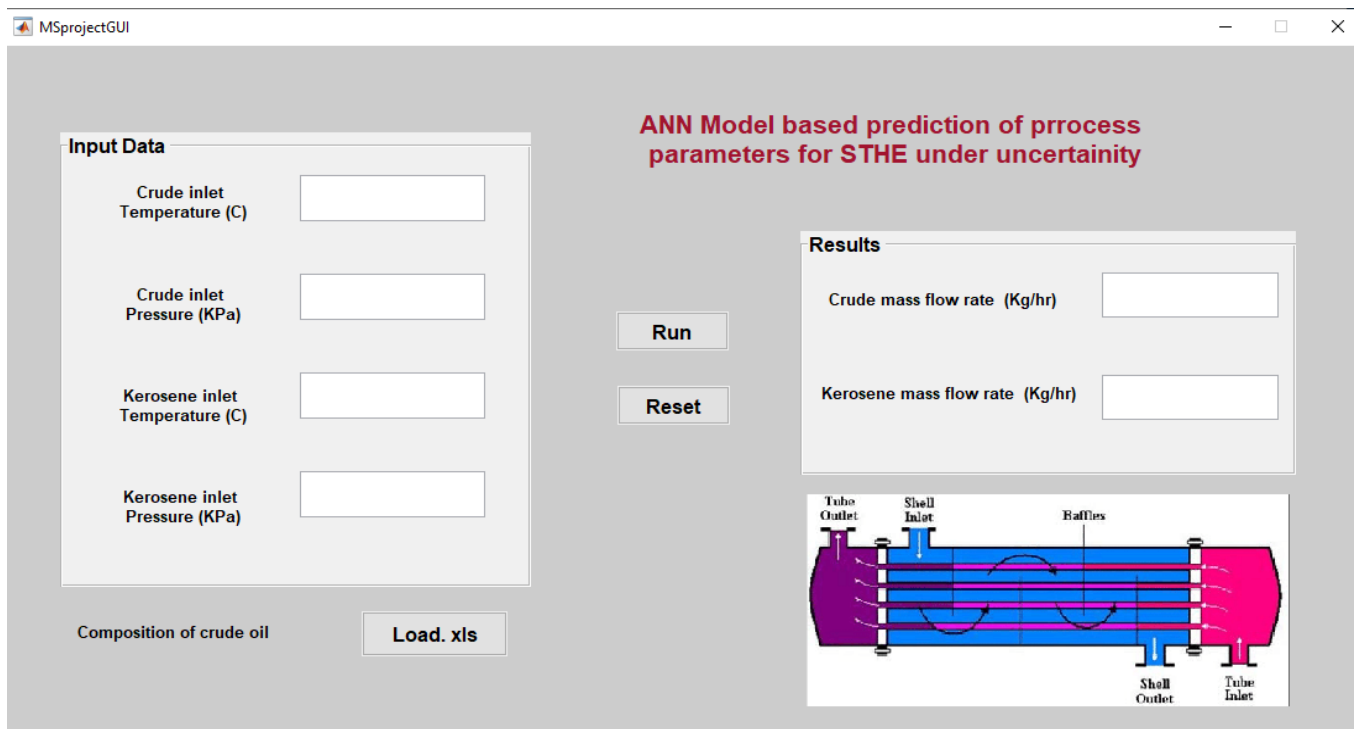


Figure 29: ANN-based Graphical user interface

CONCLUSION

Heat exchangers are used in a variety of industrial applications. Because of their complex design and high capital cost, efficient operation is critical for overall cost reduction. In this study, an ANN model was developed to predict the optimum inlet stream mass flow rates of STHE in the presence of uncertainty in the inlet Crude composition and other process conditions. The other four process variables were the inlet temperature and inlet pressure of the cold crude oil and hot kerosene oil. A total of 400 data points were generated with the help of Aspen HYSYS and MATLAB interfacing with the variation of ± 1 , ± 2 , ± 3 , ± 4 and ± 5 in the inlet crude composition and process conditions. The optimum mass flow rate for each variation was determined using a single objective genetic algorithm. The objective function for the single objective GA was to minimize the kerosene outlet temperature.

The architecture of a multi-output feed-forward neural network (MFFNN) was selected using a multi-objective GA approach. The objective function used in multi-objective GA was to select the best architecture of ANN which results in lower RMSE value. The optimized ANN framework consists of three hidden layers. The number of neurons in layers 1, 2 and 3 were 19, 18 and 20, respectively. The proposed ANN model has a high correlation coefficient of 0.999. It was discovered that the ANN model experiences the same pattern as the GA for kerosene outlet temperature and heat exchanger effectiveness. The proposed ANN model's reliable prediction and robustness will aid in lowering energy consumption and increasing equipment life by improving heat exchanger effectiveness.

FUTURE RECOMMENDATION

- The proposed method might be extended to STHes used in industries other than oil refineries for estimating optimum operating parameters under uncertainty.
- The suggested framework may be applied to various unit activities in oil refineries for efficient operation in the presence of variable process variables.
- A deep learning-based technique may also be included into the suggested framework to get more accurate findings by building a big database.

REFERENCE:

- [1] Nel W P and Cooper C J **2009** Implications of fossil fuel constraints on economic growth and global warming *Energy Policy* **37** 166–80
- [2] Yuksel I and Kaygusuz K **2011** Renewable energy sources for clean and sustainable energy policies in Turkey *Renew. Sustain. Energy Rev.* **15** 4132–44
- [3] Diya'Uddeen B H, Daud W M A W and Abdul Aziz A R **2011** Treatment technologies for petroleum refinery effluents: A review *Process Saf. Environ. Prot.* **89** 95–105
- [4] Basavarajappa S, Manavendra G and Prakash S B **2020** A review on performance study of finned tube heat exchanger *J. Phys. Conf. Ser.* **1473**
- [5] Hussein M, N.M E, Esmail E, Gadalla M and Ashour I **2021** Retrofitting Design of Heat Exchanger Networks Using Aspen-Hysys: a Case Study of Crude Oil Refining Process *J. Adv. Eng. Trends* **40** 15–22
- [6] Panahi H, Eslami A, Golozar M A and Ashrafi Laleh A **2020** An investigation on corrosion failure of a shell-and-tube heat exchanger in a natural gas treating plant *Eng. Fail. Anal.* **118** 104918
- [7] Darbandi M, Abdollahpour M-S and Hasanpour-Matkolaei M **2021** A new developed semi-full-scale approach to facilitate the CFD simulation of shell and tube heat exchangers *Chem. Eng. Sci.* **245** 116836
- [8] Yang Z, Ma Y, Zhang N and Smith R **2020** Design optimization of shell and tube heat exchangers sizing with heat transfer enhancement *Comput. Chem. Eng.* **137**
- [9] Saldanha W H, Arrieta F R P and Soares G L **2021** State-of-the-Art of Research on Optimization of Shell and Tube Heat Exchangers by Methods of Evolutionary Computation *Arch. Comput. Methods Eng.* **28** 2761–83
- [10] Kallannavar S, Mashyal S and Rajangale M **2020** Materials Today : Proceedings Effect of tube layout on the performance of shell and tube heat exchangers *Mater. Today Proc.* **27** 263–7
- [11] Jos J, Coira M L, Cruz D, Gochi C and Soares I Optimisation Techniques for Managing

the Project Sustainability Objective : Application to a Shell and Tube Heat Exchanger

- [12] Ghalandari M, Irandoost M, Akbar S, Mostafa M and Shadloo S **2021** Applications of intelligent methods in various types of heat exchangers : a review *J. Therm. Anal. Calorim.*
- [13] Armstrong M, Sivasubramanian M and Selvapalam N **2021** Experimental investigation on the heat transfer performance analysis in silver nano-coated double pipe heat exchanger using displacement reaction *Mater. Today Proc.* **45** 2482–90
- [14] Huu-Quan D, Mohammad Rostami A, Shokri Rad M, Izadi M, Hajjar A and Xiong Q **2021** 3D numerical investigation of turbulent forced convection in a double-pipe heat exchanger with flat inner pipe *Appl. Therm. Eng.* **182** 116106
- [15] Yan S R, Moria H, Pourhedayat S, Hashemian M, Assadi S, Sadighi Dizaji H and Jermstipparsert K **2020** A critique of effectiveness concept for heat exchangers; theoretical-experimental study *Int. J. Heat Mass Transf.* **159**
- [16] Shell M O F, Type T, Exchanger H, Method T, Single F O R and Optimization O
Parameter Optimization of Shell and Tube Type Heat Exchanger
- [17] Isah A, Sodiki J I and Barinyima N **2019** Performance Assessment of Shell and Tube Heat Exchangers in an Ammonia Plant *Eur. J. Eng. Res. Sci.* **4** 37–44
- [18] Taylor P, Moraga N O and López S E **2010** Numerical Heat Transfer , Part A : Applications : An International Journal of Computation and Methodology NUMERICAL SIMULATION OF THREE- DIMENSIONAL MIXED CONVECTION IN AN AIR-COOLED CAVITY 37–41
- [19] Li H and Kottke V **1998** Effect of the leakage on pressure drop and local heat transfer in shell-and-tube heat exchangers for staggered tube arrangement *Int. J. Heat Mass Transf.* **41** 425–33
- [20] Kapale U C and Chand S **2006** Modeling for shell-side pressure drop for liquid flow in shell-and-tube heat exchanger *Int. J. Heat Mass Transf.* **49** 601–10
- [21] Li H and Kottke V **1998** Visualization and determination of local heat transfer coefficients in shell-and-tube heat exchangers for staggered tube arrangement by mass transfer measurements *Exp. Therm. Fluid Sci.* **17** 210–6
- [22] Jamshidi N, Farhadi M, Ganji D D and Sedighi K 2013 Experimental analysis of heat

- transfer enhancement in shell and helical tube heat exchangers *Appl. Therm. Eng.* **51** 644–52
- [23] Butterworth D **2002** Design of shell-and-tube heat exchangers when the fouling depends on local temperature and velocity *Appl. Therm. Eng.* **22** 789–801
- [24] Coletti F and Macchietto S **2011** A dynamic, distributed model of shell-and-tube heat exchangers undergoing crude oil fouling *Ind. Eng. Chem. Res.* **50** 4515–33
- [25] Abd A A, Kareem M Q and Naji S Z **2018** Performance analysis of shell and tube heat exchanger: Parametric study *Case Stud. Therm. Eng.* **12** 563–8
- [26] Nemati Taher F, Zeyninejad Movassag S, Razmi K and Tasouji Azar R **2012** Baffle space impact on the performance of helical baffle shell and tube heat exchangers *Appl. Therm. Eng.* **44** 143–9
- [27] Akpabio E, Oboh I and Aluyor E O **2009** The effect of baffles in shell and tube heat exchangers *Adv. Mater. Res.* **62–64** 694–9
- [28] Huminic G and Huminic A **2012** Application of nanofluids in heat exchangers: A review *Renew. Sustain. Energy Rev.* **16** 5625–38
- [29] Selbaş R, Kizilkan Ö and Reppich M **2006** A new design approach for shell-and-tube heat exchangers using genetic algorithms from economic point of view *Chem. Eng. Process. Process Intensif.* **45** 268–75
- [30] Fesanghary M, Damangir E and Soleimani I **2009** Design optimization of shell and tube heat exchangers using global sensitivity analysis and harmony search algorithm *Appl. Therm. Eng.* **29** 1026–31
- [31] Fettaka S, Thibault J and Gupta Y **2013** Design of shell-and-tube heat exchangers using multiobjective optimization *Int. J. Heat Mass Transf.* **60** 343–54
- [32] Sanaye S and Hajabdollahi H **2010** Multi-objective optimization of shell and tube heat exchangers *Appl. Therm. Eng.* **30** 1937–45
- [33] Asadi M, Song Y, Sunden B and Xie G **2014** Economic optimization design of shell-and-tube heat exchangers by a cuckoo-search-algorithm *Appl. Therm. Eng.* **73** 1032–40
- [34] Hadidi A and Nazari A **2013** Design and economic optimization of shell-and-tube heat exchangers using biogeography-based (BBO) algorithm *Appl. Therm. Eng.* **51** 1263–72

- [35] Tharakeshwar T K, Seetharamu K N and Prasad B D **2017** Multi-objective optimization using bat algorithm for shell and tube heat exchangers *Appl. Therm. Eng.* **110** 1029–38
- [36] Patel V K and Rao R V **2010** Design optimization of shell-and-tube heat exchanger using particle swarm optimization technique *Appl. Therm. Eng.* **30** 1417–25
- [37] Faculty T E **2011** Design and economic optimization of shell and tube heat exchangers using Artificial Bee Colony (ABC) algorithm *β encan S* **52** 3356–62
- [38] Mirzaei M, Hajabdollahi H and Fadakar H **2017** Multi-objective optimization of shell-and-tube heat exchanger by constructal theory *Appl. Therm. Eng.* **125** 9–19
- [39] Mohanty D K **2016** International Journal of Thermal Sciences Application of fire fly algorithm for design optimization of a shell and tube heat exchanger from economic point of view *Int. J. Therm. Sci.* **102** 228–38
- [40] Xie G N, Wang Q W, Zeng M and Luo L Q **2007** Heat transfer analysis for shell-and-tube heat exchangers with experimental data by artificial neural networks approach **27** 1096–104
- [41] Duran O, Rodriguez N and Airton L **2009** Expert Systems with Applications Neural networks for cost estimation of shell and tube heat exchangers *Expert Syst. Appl.* **36** 7435–40
- [42] Thanikodi S, Singaravelu D K, Devarajan C, Venkatraman V and Rathinavelu V
TEACHING LEARNING OPTIMIZATION AND NEURAL NETWORK FOR THE
EFFECTIVE PREDICTION OF HEAT TRANSFER RATES
- [43] Hojjat M **2020** Nanofluids as coolant in a shell and tube heat exchanger : ANN modeling and multi-objective optimization *Appl. Math. Comput.* **365** 124710
- [44] Jasim H H **2013** Estimated Outlet Temperatures in Shell-and-Tube Heat Exchanger Using Artificial Neural Network Approach Based on Practical Data **9** 12–20
- [45] Carvalho C B De, Carvalho E P and Ravagnani M A S S **2018** Dynamic Analysis of Fouling Buildup in Heat Exchangers Designed According to TEMA Standards
- [46] Dqj H and Kdqj L **2020** Optimization of Shell and Tube Heat Exchangers Sizing with Heat Transfer Enhancement
- [47] Baron R and The D **2006** Multi-objective shape optimization of a heat exchanger using

- parallel genetic algorithms **49** 2567–77
- [48] Xie G N, Sunden B and Wang Q W **2008** Optimization of compact heat exchangers by a genetic algorithm **28** 895–906
- [49] Darwin C and Algorithms G *Genetic Algorithms 2.1* 15–6
- [50] Of F and Algorithm G **2008** Genetic algorithms 1–15
- [51] Wang J, Jing Y and Zhang C **2010** Optimization of capacity and operation for CCHP system by genetic algorithm *Appl. Energy* **87** 1325–35
- [52] Oyama A, Obayashi S and Nakamura T **2001** Real-coded adaptive range genetic algorithm applied to transonic wing optimization **1** 179–87
- [53] Tog V **2008** An improved genetic algorithm with initial population strategy and self-adaptive member grouping **86** 1204–18
- [54] Kaya M **2011** The effects of a new selection operator on the performance of a genetic algorithm *Appl. Math. Comput.* **217** 7669–78
- [55] Hussain A and Muhammad Y S **2020** Trade-off between exploration and exploitation with genetic algorithm using a novel selection operator *Complex Intell. Syst.* **6** 1–14
- [56] Pencheva T, Atanassov K and Shannon A 2009 1 * , 1 , 2 1 **13** 257–64
- [57] Umbarkar A J and Sheth P D **2015** CROSSOVER OPERATORS IN GENETIC ALGORITHMS : A REVIEW **6956** 1083–92
- [58] Operators A C and Applications O **1995** Per ~ tmoa ORDERING APPLICATIONS **22** 135–47
- [59] Hong T, Wang H and Chen W **2000** Simultaneously Applying Multiple Mutation Operators in Genetic Algorithms * **455** 439–55
- [60] Ahmed Z H **2015** An Improved Genetic Algorithm using Adaptive Mutation Operator for the Quadratic Assignment Problem 0–4
- [61] Isaac O, Jantan A and Esther A **2018** State-of-the-art in arti fi cial neural network applications : A survey *Heliyon* e00938
- [62] Dike H U and Zhou Y **2018** Unsupervised Learning Based On Artificial Neural Network : A Review 322–7

- [63] Benardos P G and Vosniakos G **2007** Optimizing feedforward artificial neural network architecture **20** 365–82
- [64] Abdeslam D O, Wira P and Flieller D **2007** Active Power Filters **54** 61–76
- [65] Wang J Dynamical Configuration of Neural Network Architectures 4–6
- [66] Moran M J and Sciubba E **2013** Exergy Analysis : Principles and Practice **116** 285–90
- [67] Koroneos C, Spachos T and Moussiopoulos N **2003** Exergy analysis of renewable energy sources **28** 295–310